MS No.: ESD-2015-59
Title: Observationally based analysis of land–atmosphere coupling
Author(s): F. Catalano, A. Alessandri, M. De Felice, Z. Zhu, and R. B. Myneni

Responses to Reviewers #1 and #2

First of all, we would like to thank the reviewers for their work. We found their comments helpful and we think they have given a contribution in increasing the quality of this paper. We have modified the manuscript addressing all the reviewers' requirements and suggestions and we believe that the revised manuscript is much improved.Please see below our detailed reply to the reviewers' comments.

Responses to Reviewer #1

[13/11/2015]

General comment

The paper "Observationally based analysis of land–atmosphere coupling" used the CM method to investigate the coupling relationships between soil moisture and precipitation, as well as other variables. It has some merits and presents interesting results, especially those linking EOF signals to external forcings such as ESNO and volcanic events.
The scientific question proposed regarding to land-atmosphere coupling is worth investigating, but the key content discussed in the paper is the coupling of soil moisture and precipitation, which is far form enough to cover this topic.
The authors did a lot of analysis, but unfortunately the paper is not well organized. Important information on method section is incomplete and makes it difficult to understand the following analysis and results. Overall, the presentation is not satisfactory and sometimes confusing. It lacks logic and as a reader I get lost in the too much descriptive details without a clear focus. Many key concepts like "variance" haven't been clearly defined. And language and wording is another issue that has to be significantly improved for clarity and accuracy. Although a number of Tables/figures are provided, but many of them are not very useful, they feel less informative and even hard to understand. The authors need to carefully decide how to best present their results.
It seems soil moisture does not paly a strong role as the authors claimed, because the variance of precipitation explained by soil moisture is less than 20%. Therefore, the influences of volcanic AOD as well as ENSO on PRE are relatively weak signals in general. More importantly, correlation does not necessarily mean causality or feedback, the author cited a lot of reference to explain their results, but there isn't enough information to evaluate if their proposed explanations are plausible and credible. And these discussions are mixed together with results, distracting the flow of the paper. A separate and refined discussion could be much better than current layout.
Datasets are not independent and are correlated/coupled to each other. For example, both ET and LAI are based on AVHRR. Perhaps due to this reason, precipitation forced by soil moisture is nearly equivalent to other (ET and LAI). And there are many coupling left unaccounted, e.g., soil moisture is forced by ET.
Therefore, significant efforts have to be made by the authors to address those issues relating to presentation, organization and readability of the paper before publication.

Response to general comment

We'd like to thank the reviewer for the useful comments. We revised the manuscript by addressing all his/her recommendations and we think that the revised manuscript is now much improved.

The method section has been improved to include all the relevant information and definitions, as detailed in the answers to specific comments.
The finding that, globally, 19% of precipitation (PRE) variance is forced by soil moisture (SM) indicates a significant contribution of SM on PRE variability, as also pointed out by Reviewer #2. Furthermore, locally, the ratio of PRE variance forced by SM is even larger and up to more than 30% (Fig. 2 in the paper). The identification of such hotspot regions is in good agreement with Koster et al. (2000).
We agree that correlation does not necessarily mean causality. The Coupled Manifold (CM) technique has been specifically designed to analyze covariation between climate fields considering both the local and remote forcing of one field to the other and has proved to be successful for the analysis of different climate fields, like precipitation, vegetation characteristics, sea surface temperature, and temperature over land (Alessandri and Navarra, 2008; Cherchi et al., 2007; Wang et al., 2011). To improve the robustness of the analysis we applied significance tests to the computation of the forced fields (following Cherchi et al., 2007). When discussing the feedbacks between the variables we combined the CM statistical results with a physical interpretation and literature results. We have improved the discussion of our results and how they are supported by literature in Section 4.1 (P9 L24-30 and P11 L3-7). Please see answer to minor comment 6 for more details on the advantage of CM with respect to other methods and 14 for the significance test applied in the computation of the forced fields. See also answer to general comment of Reviewer #2.
All land-surface datasets (SM, evapotranspiration [ET], Leaf Area Index [LAI]) are satellite products independent on the PRE dataset, which is based on rain gauges. It is true that both ET and LAI products have been acquired by using the AVHRR sensor but the datasets have been produced by independent research groups which used completely different methodologies. The LAI product has been generated by applying a neural network algorithm (Zhu et al. 2013) on the NDVI satellite product. The ET dataset has been produced by using a modified Penman-Monteith approach (Zhang et al. 2010) and considering eddy covariance and meteorological data from the FLUXNET towers network. This has been reported and discussed in Section 2 of the revised manuscript (P4 L18-24).
We are aware that there are interesting couplings which were not analyzed in this paper (for example, ET forcing on SM). Nevertheless, since SM has been recognized as the most important land-surface parameter affecting seasonal to interannual variability/predictability of precipitation (Koster et al., 2000; Zhang et al., 2008) we choose to focus the paper on the coupling between SM and PRE. Future papers will further address the specific coupling contribution with other fields. This has been added to Section 5 of the revised paper (P17 L3-7).

Minor comments

1) P1940 L2-3: Does the word "variance" here mean spatial or temporal variance? Need to specify.

Thank you for the comment. It is temporal variance. Indeed, the CM technique is applied to the principal components (PC) of the variables which represent the seasonal-mean inter-annual anomalies. The sentence at P1940 L2-3 has been changed in the paper as follows (P1 L15-16):
original:
"The variance of soil moisture, vegetation and evapotranspiration over land has been recognized to be strongly connected to the variance of precipitation."
new:
"The temporal variance of soil moisture, vegetation and evapotranspiration over land has been recognized to be strongly connected to the temporal variance of precipitation."

2) L6: what does "memory" means here? I don't get it.
Thanks. The term "memory" refers here to the property of some variables characteristics of slowly varying components of the Earth system to display persistent anomalies induced by climatic events like ENSO or volcanic eruptions (Koster et al., 2000). Since slowly varying states of the land surface can be predicted weeks to months in advance, the response of the atmosphere to these land-surface anomalies can contribute to seasonal prediction (Alessandri and Navarra, 2008). This explanation has been added to Section 1 of the revised paper. See response to comment 3.

3) P1941 L11 Please explain "soil moisture memory".
Thanks for the suggestion. Please see response to point 2. The expression "soil moisture memory" has been used in literature (Koster et al., 2004; Ferranti and Viterbo, 2006). To better clarify the expression, the following phrase has been added to Section 1 of the revised manuscript (P2 L21-25):
"The term "soil moisture memory" refers here to the property of soil moisture to display persistent anomalies induced by climatic events like ENSO or volcanic eruptions. Since slowly varying states of the land surface can be predicted weeks to months in advance, the response of the atmosphere to these land-surface anomalies can contribute to seasonal prediction."

4) L22 "improvement" of what?
Thanks. To clarify it, the phrase has been modified as following (P3 L3-4):
original:
"However, much of the improvement so far has been obtained over ocean"
new:
"However, much of the model improvements so far have been obtained over ocean..."

5) P1942L9 what does "land variability" indicate here?
The term "land variability" indicates here the seasonal-mean inter-annual variability of land-surface variables (SM, ET, LAI). The phrase has been modified in the text as follows (P3 L18-19):
original:
"The comprehensive dataset is analysed to characterize the land variability and..."
new:
"The comprehensive dataset is analysed to characterize the seasonal-mean inter-annual of land-surface variables (SM, ET, LAI) and..."

6) L13-L20 what is advantage of CM method compared to other methods?
Thank you for the question. The following phrase has been added to Section 3 of the revised manuscript to explain the advantage of CM with respect to other methods (P6 L17-24):
"There are two main advantages of the CM method. The first one is that, when applied to a couple of climate fields (i.e., PRE and SM), CM is able to separate one field (i.e., PRE) into two components: the first component (forced) is the portion of PRE variability that is connected to the SM variability, whereas the second (free) is the part of PRE that is independent from SM. Therefore, the CMT enables to find robust relations between fields in the presence of strong background noise. The second advantage is that the CM technique is able to detect both local and remote effects of the forcing variable. This is not possible with other methods such as SVD (Singular Value Decomposition)."

7) P1943 L4 It is strange for me to see the claim that those datasets are "state-of-art". For example, there are many alternative precipitation, ET and LAI datasets and it is hard to say one is better than the other without rigorous comparison. The data used here are far from "state-of-art". As far as I know, GLEAM ET and GLASS LAI are also high quality products.
We agree with the reviewer that there exist other high quality datasets of ET, LAI and PRE. A rigorous comparison of recent land-surface datasets is well beyond the scope of our paper. We based the choice of the datasets for our analysis mainly on two criteria: 1) the period covered has to be as long as possible; 2) the spatial coverage has to be global. We have discussed this in Section 2 of the revised paper (P4 L10-12). In order to avoid confusion, in the revised manuscript we changed the term "state-of-the-art" with "high quality".

8) L20 Please briefly explain the gap filling procedure used.
Thanks. The procedure is described in Section 3 of the manuscript, as follows:
"The LAI and SM datasets contain missing values, whose number and position significantly vary with time. The application of the CM algorithms requires that the number and position of the missing values is constant with time. Hence, if a NaN is present in a given grid-point at any time, then it requires to mark as NaN that grid point, thus losing a great amount of information. In order to keep as much information as possible from the data, we decided to replace the missing values with climatological values provided that their total number, considering a particular grid-point, does not exceed a given threshold. We selected different thresholds for SM and LAI in order to obtain as similar as possible spatial coverage of the two variables. The chosen threshold is 10 % for LAI and 30 % for SM. The results are robust with respect to a ±10 % change of the threshold values."
The following sentence which points to the explanation is further added to Section 2 of the revised manuscript (P4 L31-32):
"The gap filling procedure is described in Section 3."

9) L22 The use of model information weakens the previous claim that these observation data are independent of models.
We agree with the reviewer that the observational datasets have been derived based on limitations and constraints. The use of model information for ET and PRE datasets is declared in Section 2. To clarify the point raised by the reviewer, we have modified the following sentence at the beginning of Section 2 of the revised manuscript (P4 L6):
original:
"...in order to make the analysis as much as possible independent from numerical model limitations and biases..."
new:
"...in order to make the analysis as much as possible independent from global circulation models limitations and biases..."

10) Table 1. Better to add Ref for each dataset shown in the table; and spell out ET, LAI, GPCP etc. or explain them in notes.
We appreciate the suggestion. In the revised manuscript we have recalled the dataset references in the table caption. We have also added the extended name of the datasets in caption.

11) P1944 The authors at least need to describe the mathematical theory of CM (Eq. 1 and 2) and explain how it works to decompose a field into forced and free components.
Thanks. The mathematical theory of CM is described in detail in the cited reference of Navarra and Tribbia (2005). In order to better explain the rationale of the CM method we added the following sentence to Section 3 of the revised manuscript (P5 L30-P6 L2):
"A and B are found by solving the Procrustes minimization problem:

A=ZS'(SS')^-1 (3)
B=SZ'(ZZ')^-1 (4)"
Following equations have been renumbered accordingly.

12) L18 what is CCA scaling?
Thanks. CCA scaling is data scaled by the covariance matrices. This is now explained in Section 3 of the revised manuscript, by changing the following sentence (P6 L5):
original:
"CCA scaling is applied to the Principal Components..."
new:
"CCA scaling (data scaled by the covariance matrices) is applied to the Principal Components..."

13) Since Eq 3 and 4 are listed in method, the authors must explain their meanings. What are Z^ and S^? And I don't understand why Eq 3 and 4 are needed here?
We appreciate the suggestion. Z^ and S^ are the CCA-scaled variables. Please see also response to comment 12. Eqs. 3 and 4 are the mathematical expression of the CCA scaling. This has been specified in the revised manuscript by adding the following sentence in the revised manuscript (P6 L10):
"where Z^ and S^ are the CCA-scaled variables."
For further details on the CCA scaling technique we refer to Navarra and Tribbia (2005).

14) P1945 L1-3. How to understand significance level for each element in A and B?
Thanks. This has been better explained in the revised manuscript, by adding the following sentence (P6 L12-14):
"As explained in Cherchi et al. (2007), after applying the CCA scaling, the elements of A and B are correlation coefficients and can be tested (with a significance test based on the Student t distribution) to reject the null hypothesis of being equal to zero."
The following sentence is further modified in the revised manuscript (P 6 L16):
original:
"...at the 1 % level significance level..."
new:
"...at the 1 % significance level..."

15) L6-8 Why not to follow the common practice to define four seasons as JJA, SON, DJF and MAM? The incompatible definition for season would make this study incomparable with most other studies.
Thanks for the comment. We chose this definition for seasons because most of the datasets we use start on January and with the DJF, MAM, JJA, SON stratification we would have had to discard the first incomplete winter season and because the JFM, AMJ, JAS, OND stratification has been used by Alessandri and Navarra (2008) in their CM study of vegetation and rainfall which we used to compare our results. We have discussed this by adding the following sentence in the revised manuscript (P6 L28-P7 L1):
"The JFM, AMJ, JAS, OND stratification has been used by Alessandri and Navarra (2008) in their CM study of vegetation and rainfall which we will use to compare our results.

16) L10-20. It seems this paragraph describes the gap filling method?
Thanks. We now point to this paragraph in Section 2 of the revised manuscript. Please see response to comment 8.

17) L23 EOF is an important part for the analysis but has never been explained previously in the method section.
Thank you for the suggestion. We have modified the sentence in the revised manuscript to include EOF definition (P7 L22-23):
original:
"interpretation of the EOF patterns"
new:
"...interpretation of the Empirical Orthogonal Functions (EOF) patterns (Bretherton et al., 1992)..."
The following reference has been added to the revised manuscript (P18 L16-17):
Bretherton, C. S., Smith, C., and Wallace, J. M.: An intercomparison of methods for finding coupled patterns in climate data. J. Climate, 5, 541-560, 1992.

18) P1946 L3 Again, what is "variance" here? Is it temporal or spatial variance?
Thanks for the comment. It is temporal variance. Please also see response to comment 1.

19) L1-L14. It seems all these variables are coupled with each other in multiple ways, e.g., ET and LAI, LAI and SM, and ET and SM are correlated/interconnected but not analyzed here. According to Table 2, LAI and ET have similar role on PRE compared to SM. Despite PRE, LAI and ET are also important drivers for SM and may also accounts for a fraction of variance of SM.
We agree with the reviewer that it would be interesting to analyze in detail the reciprocal forcings between ET and LAI, LAI and SM and ET and SM. Nevertheless, since SM has been recognized as the most important land-surface parameter affecting seasonal to interannual variability of precipitation (Koster et al., 2000; Zhang et al., 2008) we choose to focus the paper on the coupling between SM and PRE. We plan to write a follow-up paper that will further address the specific coupling contribution with other fields. This has been added to Section 5 of the revised paper (P17 L3-7).

20) P1947 L1-3 how to define transitional regions, are there any quantitative criteria for that?
There are no unique quantitative criteria. Here we refer to the transition zones between very dry and very humid environments, where ET is very sensitive to SM, as individuated by Koster et al. (2000). This has been specified in Section 4.1 of the revised manuscript (P8 L22-23).

21) Table 3 uses Rainfall but in the text that is PRE. The use of term must be consistent throughout the paper to avoid possible confusion. And NINO3 in the table should be explained.
Thanks. We changed "rainfall" to "PRE" in table caption and we recalled in the caption the definition of the NINO3 index "(average of the Sea Surface Temperature in the tropical Pacific region 5◦ S–5◦ N, 210–270◦ E)".

22) L6 In table 2, SM only accounts for 17% variance of PRE, why EOF shows 48% of total variance in table 3?
In table 2, SM accounts for 19% variance of PRE. In table 3, we list the variance explained by each mode of the PRE forced field. 48% is the variance explained by the first 3 modes of PRE forced by SM. This sentence has been added to the revised manuscript (P8 L26-28):
"The variance explained by each mode of the PRE forced field is reported in Table 3."

23) L12 All data used including AOD should be descripted in method section.
Thanks for the comment. We added a brief description of the AOD and SST datasets at the end of Section 2 of the revised manuscript, as also suggested also by Reviewer #2 (P5 L14-18):
"In order to evaluate the effect of major volcanic eruptions on land-atmosphere coupling, we used the stratospheric Aerosol Optical Depth (AOD) at 550 nm, available from the NASA GISS

dataset (Sato et al., 1993). To evaluate the effect of ENSO, we compute the NINO3 index based on the HadISST 1.1 – Global sea-Ice coverage and Sea Surface Temperature (1870–present; Rayner et al., 2003) dataset."
The following reference has been added to the revised manuscript (P20 L19-20):
Sato, M., Hansen, J. E., McCormick, M. P., and Pollack, J. B.: Stratospheric aerosol optical depth, 1850-1990. J. Geophys. Res. 98, 22987-22994, 1993.

24) I am confused by Table 3 and Table 4 that show different variance explained by PCs.
Table 3 shows the variance explained by each EOF mode of the PRE component which is forced by SM. On the other hand, Table 4 reports the variance explained by each EOF mode of the whole original PRE field (that is, forced+free components). The sentence has been added to the revised manuscript (P9 L14-15).

25) P1950 L18-24 and Table 5: How to understand "PRE forced by SM and ET(LAI)". Do they mean PRE forced by SM is further decomposed into two parts - forced by ET and free? The corresponding text is not clear enough to correctly get the meaning. My understanding is that in this case, 17% x 20% = 3.4%, does it suggest only 3.4% PRE variance is explained by ET? ET and LAI are closely related especially in vegetated areas as the calculation of ET may have used LAI. This can be seen in the similar distribution of identified hotspots.
Thanks for the comment. We modified the following sentence in the revised manuscript to clarify the procedure (P11 L32-P12 L1):
original:
"...we applied the CM technique between PRE forced by SM and ET (LAI)..."
new:
"...we further applied the CM technique between the components of PRE forced by SM and ET (LAI)..."
We found that 19% of PRE variability is forced by SM (Table 2). On the other hand, ET explains 20% of the variability of PRE forced by SM. We further added the following sentence to the revised paper (P12 L4-7):
"It is important to note here that 19%x20%=3.8% represents only the ET forcing on PRE mediated by SM and not the whole ET forcing on PRE which is actually 18% (Table 2). At the same time, 23% of the variance of PRE forced by SM is evaluated to be also forced by LAI, therefore the LAI forcing on PRE mediated by SM corresponds to 17%x23%=3.9%."

26) P1951 The analysis in the second paragraph is very difficult to follow! And I don't quite understand the explanations that linking ET to AOD.
We have added the following sentence in Section 4.2 (P12 L21-25):
"Here we take the physical fields corresponding to the first three modes of variability of PRE forced by SM and further decompose them to extract the parts of each mode that is forced by ET and LAI, respectively. This analysis allows to figure out how ET and LAI contribute to each component of PRE forced by SM which has been identified to be linked to external climate forcing (volcanic eruptions, ENSO and a trend)."
Eventually, we apply the CM to find the components of PRE forced by ET and LAI, respectively (Table 7) and we show that we can find the same link with external climate forcings in the EOFs. This confirms the robustness of the signals we found in the EOFs of PRE forced by SM and the lagged correlation with AOD shown in Table 7 indicates that ET and LAI contribute to extend the land-surface "memory" of the volcanic eruptions. In the case of ET, we found that this variable explains 21% of the variance of the first mode of PRE forced by SM (linked to AOD). Volcanic signal is found also in the third PC of PRE forced by ET, indicating a mediation role of ET in the response of PRE forced by SM to volcanic eruptions.

27) The direction of triangles in Figure 7 is almost indistinguishable without zooming.
Thanks for the comment. We have improved Figs. 7, 8, 9a,b by using larger markers.

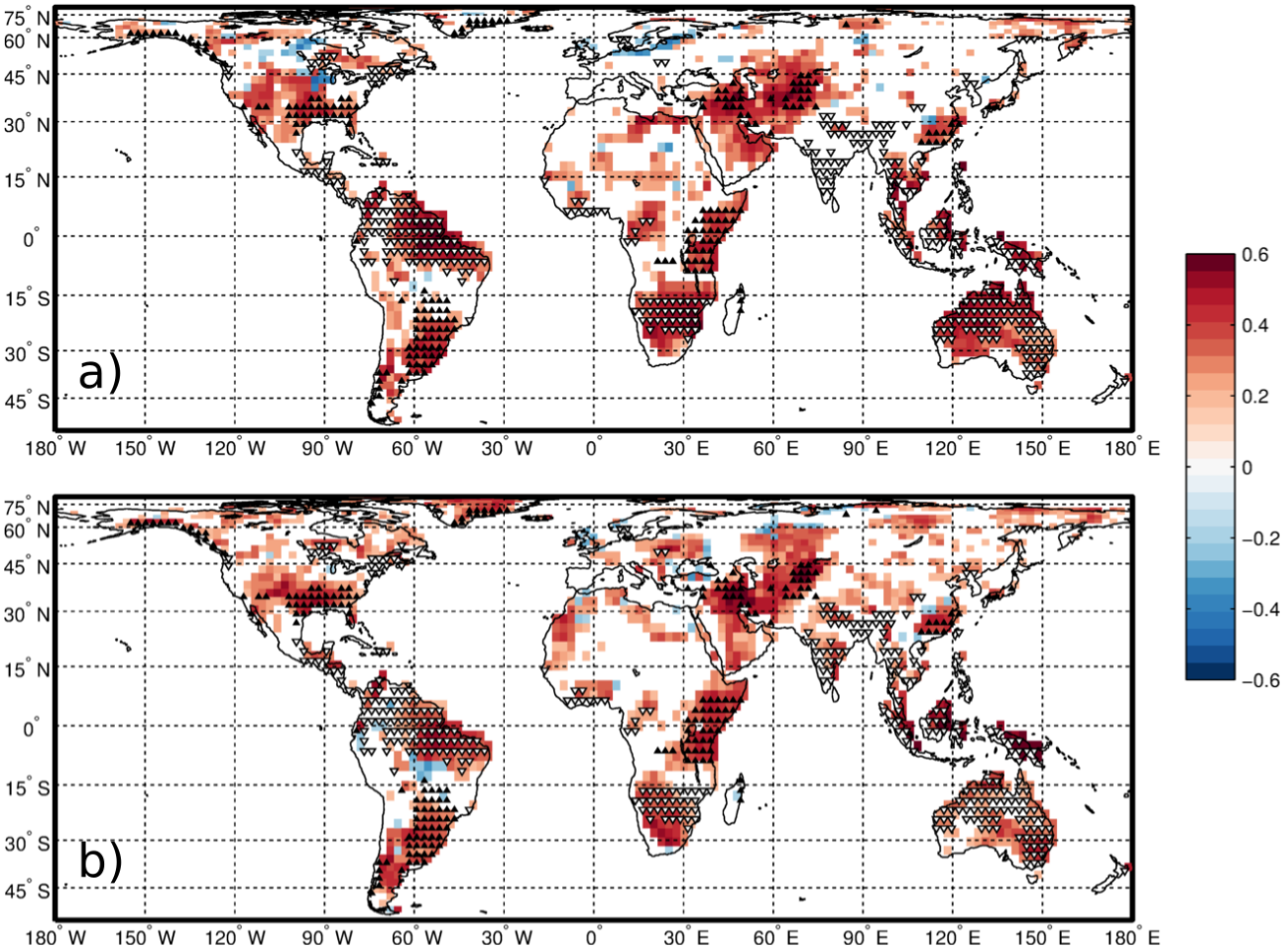

new Fig. 7.

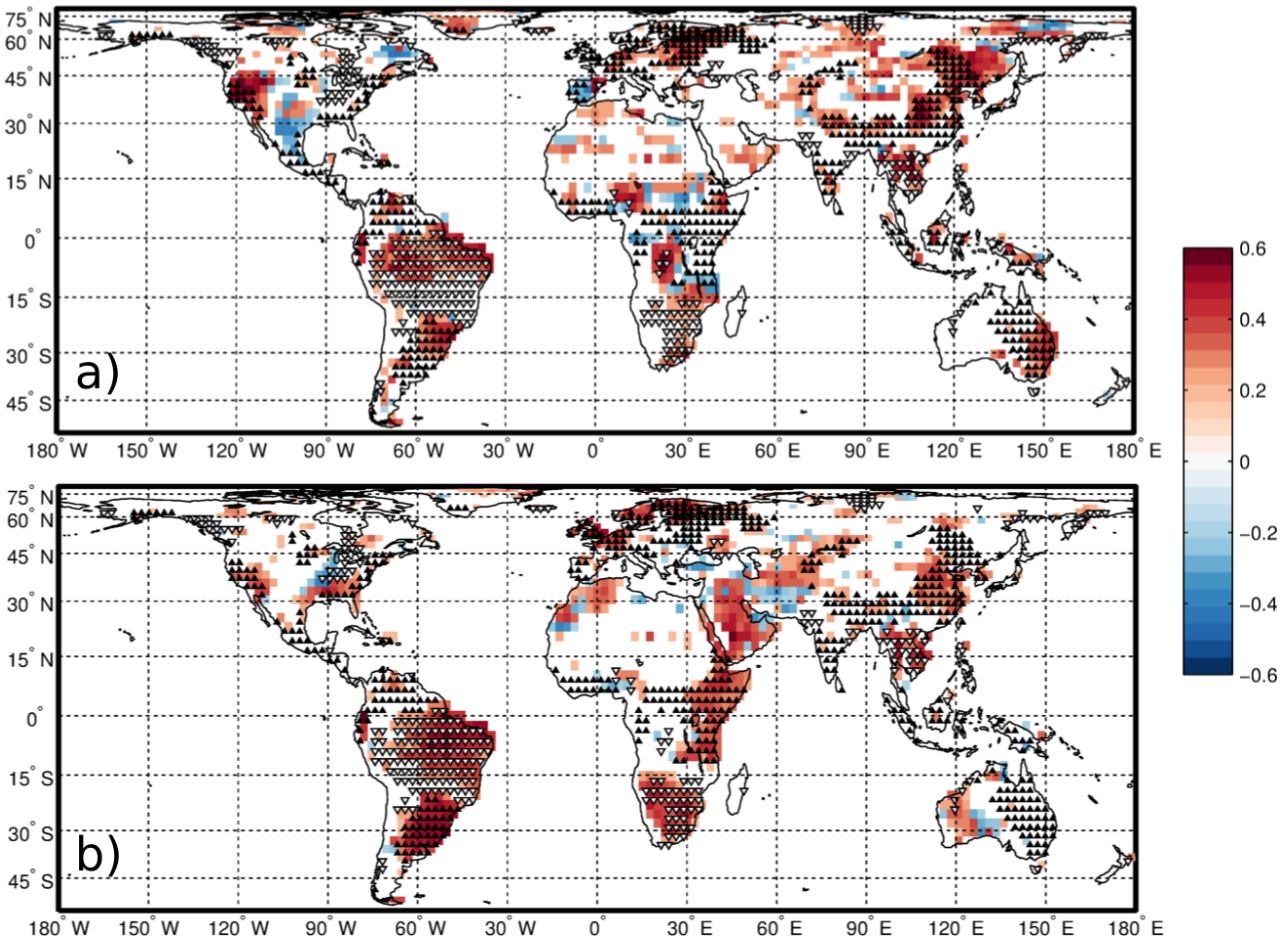
75° N
60° N
45° N
30° N
15° N
0°
15° S
30° S
45° S
a)
180° W
150° W
120° W
90° W
60° W
30° W
0°
30° E
60° E
90° E
120° E
150° E
180° E
b)
0.6
0.4
0.2
0
−0.2
−0.4
−0.6
new Fig. 8.

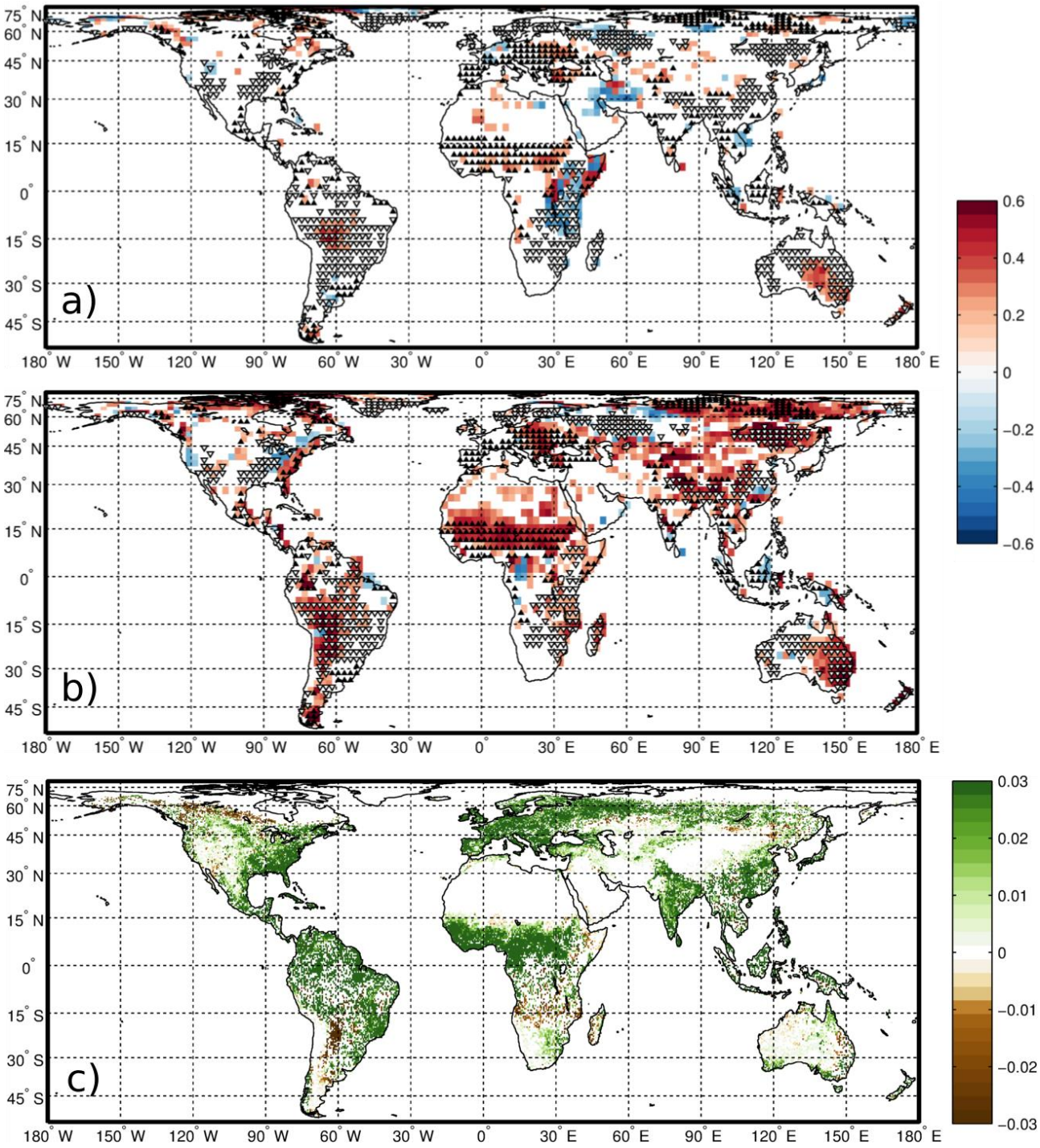
a)
b)
c)
75° N
60° N
45° N
30° N
15° N
0°
15° S
30° S
45° S
180° W
150° W
120° W
90° W
60° W
30° W
0°
30° E
60° E
90° E
120° E
150° E
180° E
0.6
0.4
0.2
0
−0.2
−0.4
−0.6
0.03
0.02
0.01
0
−0.01
−0.02
−0.03

new Fig. 9.

Responses to Reviewer #2

[05/01/2016]

General comment

The manuscript "Observationally based analysis of land–atmosphere coupling" by Catalano et al. has analysed the covariation between satellite derived observationally based monthly precipitation, soil moisture, evapotranspiration and leaf area index using the coupled manifold technique, which considers both the local and remote forcing of one field to the other. This generalized linear method is used to assess the reciprocal forcing of seasonal mean land surface variables and precipitation anomalies over land.

This is an interesting study providing new insights on the understanding of the land surface atmosphere feedbacks by quantifying the linear coupling between the land surface variables and the climate. The finding that 19% of the inter-annual variability of the precipitation over continental areas is forced by the SM variation is useful new information. The analysis also reveals that the dominant components of the SM forced precipitation variability are the volcanic eruptions and ENSO.

However the finding using the stratospheric AOD estimates that the aerosol emitted during the volcanic eruptions has the effect of reducing the intensity of precipitation over areas of wet climate is not well supported by the cited references, for example, the statement on page 1948, line 6 referring to Alessandri et al., (2012) and the discussion in page 1948, line 6 "the negative signal over India may indicate a suppression of the monsoon linked to the effects of the aerosol released during major eruptions according to Iles et al. (2013)" contradicts IIes et al. finding that HadCM3 precipitation response to volcanic eruptions exhibit drying in monsoon regions except India. The finding that the second dominant component of the precipitation variability forced by SM indicates positive precipitation anomalies over South India related to the positive phase of ENSO also need to be clarified as most of the previous research has found reduced precipitation over India during ENSO years.

The data gaps in the satellite derived SM and LAI are replaced at many grid points with climatological values for applying the CM technique. Figure 1 shows that the seasonal cycle of the percentage of number of grid points replaced globally for SM ranges from 28 to 48%. It is suggested that a figure can be added with the grid point locations using climatological SM values marked so that how much the missing SM data has influenced the major findings of this study can be discussed and highlighted in the abstract.

Overall the paper is well written, structured and referenced. The abstract reflect the content of the paper and provide a clear and complete summary. I recommend its publication after the minor issues mentioned above are addressed.

Response to general comment

We would like to thank the reviewer for the useful comments. We followed all the reviewer recommendations and we think the discussion in the revised paper is now much improved.

We have changed the discussion of the effect of the aerosol on precipitation on page 1948 to make it consistent with the literature cited (P9 L24-30).

Original:

"In particular, the negative signal over India may indicate a suppression of the monsoon linked to the effects of the aerosol released during major eruptions according to Iles et al. (2013)."

new:

"In particular, according to Joseph and Zeng (2011) and Iles et al. (2013), the negative signal over the monsoon regions may indicate a suppression of the monsoon linked to the effects of the aerosol released during major eruptions. Furthermore, differently from our results and other observational

(Trenberth and Dai, 2007) and modelling (Joseph and Zeng, 2011) studies, the HadCM3 results of Iles et al. (2013) showed a wetting signal over India during the summer season (although not significant in the observational dataset they used)."
With respect to the relation between the second mode of variability and ENSO, we are grateful to the Reviewer for having evidenced this interesting negative feedback. We have added the following sentence in the revised manuscript (P11 L3-7):
"Most previous research showed reduced precipitation over India during ENSO years (Ropelewski and Halpert, 1989; Trenberth et al., 1998). The positive anomalies of PRE forced by SM over South India related to the positive phase of ENSO evidence an interesting negative feedback of the land-surface on the effect of ENSO on the rainfall over India."

The following new reference has been added to the revised manuscript (P19 L13-14):
Joseph, R., and Zeng, N.: Seasonally modulated tropical drought induced by volcanic aerosol, J. Clim., 24(8), 2,045–2,060, doi:10.1175/2009JCLI3170.1, 2011.

As suggested, in order to better evaluate and discuss how the missing SM data has influenced the major findings of the study we have added a panel in Fig. 1 with a map of the percentage of SM missing data for each grid point. We recall here that all grid points with a percentage of missing number larger than 30% have been discarded (white areas in Fig. 1b). The following sentence has been added to Section 2 (P5 L8-10):
"Fig. 1b shows the percentage of SM missing data for each grid point. All grid points with a percentage of missing number larger than 30% (white areas in Fig. 1b) have not been considered in the analysis."
The following sentence has been further added to Section 3 (P7 L12-19):
"As shown in Fig. 1b, the areas more affected by the replacement of SM missing values (30% of values replaced by climatology) are North-East Europe, East coast of Central-South America, East China and Korea. Since the replacement of missing values with climatology reduces time variability, the coupling in these regions may be underestimated as a consequence. We note that these gap-filled regions do not correspond to transition zones between wet and dry climates (Koster et al. 2000). Therefore, they are not expected to display a strong coupling between SM and PRE and to significantly affect the main results of present study."

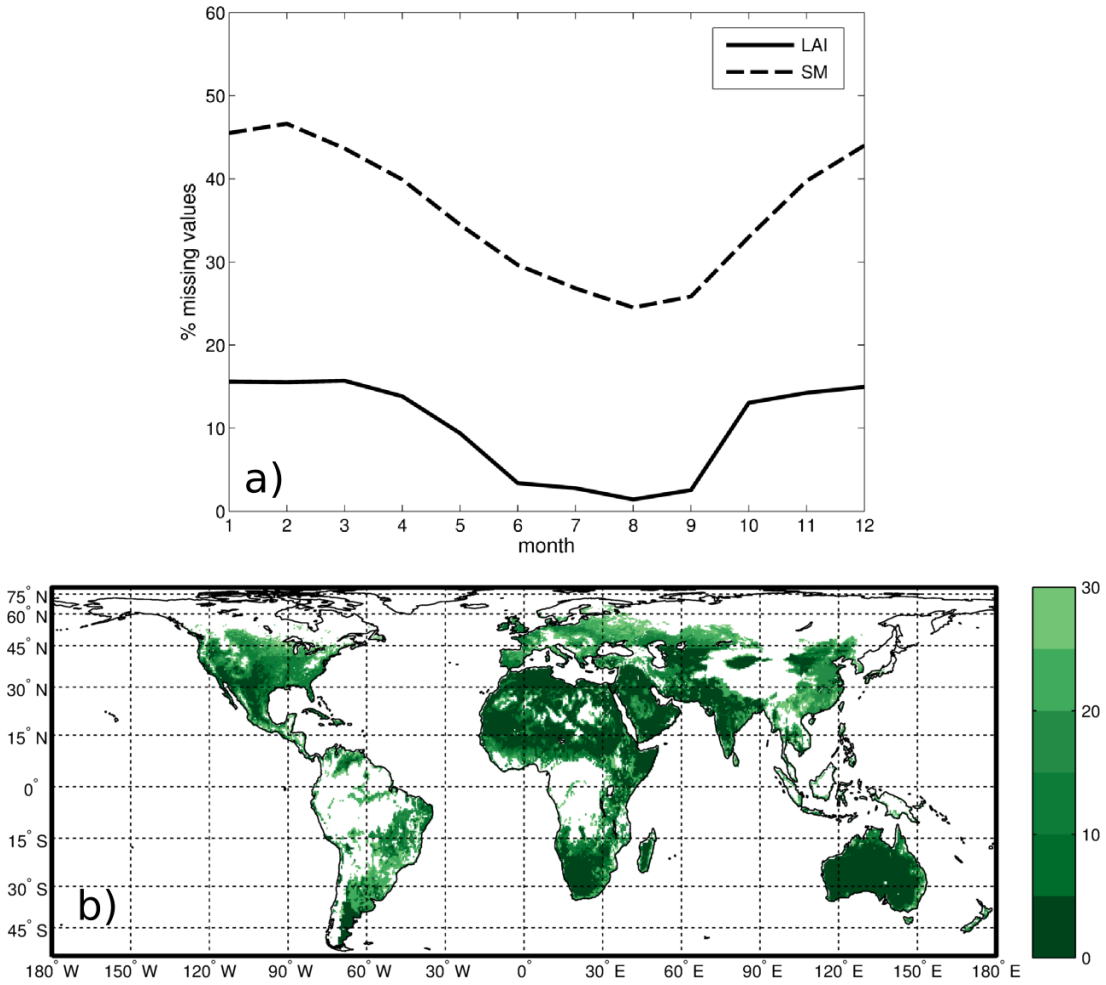

new Fig. 1.

Minor comments

1) P1947;L13: Please provide details of the stratospheric AOD dataset with relevant references in the Dataset section.
Thanks for the comment. We added a brief description of the AOD and SST datasets in Section 2 of the revised manuscript (P5 L14-18). See also answer to minor comment 23 of Reviewer #1.

2) P1948;L1 and P1949;L12: Replace "horizontal" with "spatial".
Thanks. Changed as suggested in the revised manuscript.

3) P1948;L26: The description of the HadISST dataset may be moved to the Dataset section.
Done. Thanks for the suggestion. Please see also response to comment 1.

Observationally based analysis of land-atmosphere coupling

F. Catalano[1], A. Alessandri[1], M. De Felice[1], Z. Zhu[2,3] and R. B. Myneni[4]

[1]{Italian National Agency for New Technologies, Energy and Sustainable Economic Development (ENEA), Rome, Italy}

[2]{State Key Laboratory of Remote Sensing Science, Institute of Remote Sensing and Digital Earth, Chinese Academy of Sciences, Beijing, China}

[3]{Center for Applications of Spatial Information Technologies in Public Health, Beijing, China}

[4]{Department of Earth and Environment, Boston University, Boston, MA, USA}

Correspondence to: F. Catalano (franco.catalano@enea.it)

Abstract

The temporal variance of soil moisture, vegetation and evapotranspiration over land has been recognized to be strongly connected to the temporal variance of precipitation. However, the feedbacks and couplings between these variables are still not well understood and quantified. Furthermore, soil moisture and vegetation processes are associated to a memory and therefore they may have important implications for predictability.

In this study we apply a generalized linear method, specifically designed to assess the reciprocal forcing between connected fields, to the latest available observational datasets of global precipitation, evapotranspiration, vegetation and soil moisture content. For the first time a long global observational dataset is used to investigate the spatial and temporal land variability and to characterize the relationships and feedbacks between land and precipitation.

The variables considered show a significant coupling among each other. The analysis of the response of precipitation to soil moisture evidences a robust coupling between these two variables. In particular, the first two modes of variability of the precipitation forced by soil moisture appear to have a strong link with volcanic eruptions and ENSO cycles, respectively,

and ~~that~~ these links are modulated by the effects of evapotranspiration and vegetation. It is suggested that vegetation state and soil moisture provide a biophysical memory of ENSO and major volcanic eruptions, revealed through delayed feedbacks on rainfall patterns. The third mode of variability reveals a trend very similar to the trend of the inter-hemispheric contrast in SST and appears to be connected to greening/browning trends of vegetation over the last three decades.

1 Introduction

Soil moisture (SM) is an important variable of the climate system, playing an important role in the feedbacks between land-surface and atmosphere. SM is important in determining climate variability at a wide range of temporal and spatial scales and controls hydrologic and energy cycles (Seneviratne et al., 2010; Dirmeyer, 2011). Soil moisture-precipitation feedbacks have been investigated at the global (Koster et al., 2004; Koster et al., 2009) and the regional (Pal and Eltahir, 2003; Hohenegger et al., 2009) scale through numerical simulations. Recent observational studies focused on local land-atmosphere coupling (Santanello et al., 2009). However, a comprehensive observational study at the global scale of the SM precipitation (PRE) coupling has never been performed. As shown by several modelling studies, it is over transition zones between wet and dry climates that a strong coupling between soil moisture and precipitation can be clearly identified and it is over these regions that "soil moisture memory" can most probably contribute to subseasonal and longer climate predictions (Koster et al., 2004; Ferranti and Viterbo, 2006). The term "soil moisture memory" refers to the property of soil moisture to display persistent anomalies induced by climatic events like ENSO or volcanic eruptions. Since slowly varying states of the land surface can be predicted weeks to months in advance, the response of the atmosphere to these land-surface anomalies can contribute to seasonal prediction. T~~Nevertheless, t~~he large discrepancies among model results evidence the need of observational analysis of soil moisture-precipitation feedbacks (Seneviratne et al., 2010). The observational study by Alessandri and Navarra (2008) clearly identified a link between rainfall and land surface-vegetation variability indicating an important delayed feedback of the land surface to the precipitation pattern. In this regard, a mechanism by which vegetation may provide delayed memory of El Niño and La Niña events is identified.

Predictability of climate at seasonal and longer time scales stems from the interaction of the atmosphere with slowly varying components of the climate system such as the ocean and the land surface (Shukla and Kinter, 2006). However, much of the model improvements so far haves been obtained over ocean, where extensive availability of observations allowed model progresses and reliable application of assimilation techniques (Rosati et al., 1997; Alessandri et al., 2010; Alessandri et al., 2011). In contrast, forecasts performance over land is substantially weaker compared to the ocean (Wang et al., 2009; Alessandri et al., 2011). Since most of the applications of climate predictions would serve economic interests that are land-based, there is an urgent need to improve climate forecasts over land. Long-term improvements in understanding land-climate interactions and feedbacks over land must come from the enhancement of the description of the physical processes on the basis of dedicated process studies and observational databases. This can be suitably pursued firstly by analysing the newest available satellite-derived observational datasets that can lead to a better understanding and quantification of land surface-atmosphere feedbacks. The better knowledge will then help us to conceive improved systems for the simulation of climate and for the improvement of its prediction at seasonal and possibly longer time scales. Here a global array of relevant up-to-date state-of-the-arthigh quality datasets is acquired, harmonized and analysed. The comprehensive dataset is analysed to characterize the seasonal-mean interannual land variability of land-surface variables and to improve understanding of the relationship and feedbacks between land and climate. The analysis method is based on the Coupled Manifold (CM) technique (Navarra and Tribbia, 2005) which has been specifically designed to analyse covariation between fields considering both the local and remote forcing of one field to the other. The CM has proved to be successful for the analysis of different climate fields, like precipitation, vegetation characteristics, sea surface temperature, and temperature over land (Alessandri and Navarra, 2008; Cherchi et al., 2007; Wang et al., 2011). Recently, the CM technique has been also applied to investigate the relationship between surface temperature and electricity demand in summer (De Felice et al., 2014). By taking advantage of the new global array of relevant up to date state-of-the-arthigh quality datasets, the present work substantially extends the analysis previously performed by Alessandri and Navarra (2008) and, for the first time, it includes SM and evapotranspiration (ET) feedbacks on PRE.

This paper is organized as follows: the observational datasets are described in Section 2. Section 3 describes the analysis method and gives a brief introduction of the CM technique.

Section 4 presents the results. Summary and discussion of the main results of this study are given in Section 5.

2 The observational datasets

The datasets used for this study are all observationally based, in order to make the analysis as much as possible independent from global circulation~~numerical~~ model limitations and biases. ~~State-of-the-art~~High quality up-to-date observational datasets of precipitation (PRE, from the Global Precipitation Climatology Project [GPCP]), Evapotranspiration (ET, from University of Montana), soil moisture (SM, from European Space Agency [ESA]) and Leaf Area Index (LAI, from Boston University) have been acquired and prepared. The selection of the datasets is based mainly on two criteria: 1) as long as possible period covered; 2) global spatial coverage. The observed monthly PRE dataset is described in Adler et al. (2003). ET values are satellite-based estimates from the Global Inventory Modeling and Mapping Studies [GIMMS] and MODIS (Zhang et al., 2010). The SM dataset (Liu et al., 2011, 2012) is the most complete record of this variable, based on active and passive microwave satellite sensors. The LAI dataset (Zhu et al., 2013) is a long-term global data set resulting from the application of a neural network algorithm to the NDVI3g product from GIMMS satellite data. All land-surface datasets (SM, ET, LAI) are satellite products independent on the PRE dataset, which is based on rain gauges. Despite both ET and LAI products have been acquired by using the AVHRR sensor, the datasets have been produced by independent research groups which used completely different methodologies. The LAI product has been generated by applying a neural network algorithm on the NDVI satellite product while the ET dataset has been produced by using a modified Penman-Monteith approach including eddy covariance and meteorological data from the FLUXNET towers network. The time period, depending from the availability of the datasets, is 24 years (1983-2006) for ET and 29 years (1982-2010) for the other variables. Original datasets come with various sampling frequencies, ranging from daily to monthly. See Table 1 for a summary of the characteristics of the retrieved datasets.

The data have been pre-processed and prepared for the subsequent analysis (Table 1). The pre-processing included space and time averaging, analysis of the spatial coverage and gap filling in order to minimize the effect of undefined values (hereinafter NaN). The gap filling procedure is described in Section 3. ET and PRE datasets are observational products merged

with model information and so do not contain NaNs. Instead, LAI and SM are affected by data gaps and present significant seasonal variation of the spatial coverage. Fig. 1a reports the seasonal cycle of the percentage of NaN values for LAI (full line) and SM (dashed line). Both variables show better spatial coverage during the summer season (June, July, August, September). On the other hand, mostly because satellite-based estimates of LAI and SM are unreliable in presence of snow cover (Zeng et al., 2013), during the winter season the coverage reduces substantially. The SM dataset derives from blending passive and active microwave satellite retrievals. Fig. 1b shows the percentage of SM missing data for each grid point. All grid points with a percentage of missing number larger than 30% (white areas in Fig. 1b) have not been considered in the analysis. Over regions characterized by particularly dense vegetation and high canopies, both satellite products are unable to provide reliable estimates (Liu et al., 2012). Conversely, non-vegetated areas are associated to NaN values in the LAI dataset.

In order to evaluate the effect of major volcanic eruptions on land-atmosphere coupling, we used the stratospheric Aerosol Optical Depth (AOD) at 550 nm, available from the NASA GISS dataset (Sato et al., 1993). To evaluate the effect of ENSO, we compute the NINO3 index based on the HadISST 1.1 – Global sea-Ice coverage and Sea Surface Temperature (1870–present; Rayner et al., 2003) dataset.

3 The Analysis Method

The CM technique (Navarra and Tribbia, 2005) seeks linear relations between two atmospheric fields Z and S (that in general are assumed to be rectangular matrices) of the kind:

$$Z = Z_{for} + Z_{free} = AS + Z_{free}, \quad (1)$$

$$S = S_{for} + S_{free} = BZ + S_{free}, \quad (2)$$

The subscript $()_{for}$ indicates the component of the field forced by the other variable (hereinafter forced manifold), while $()_{free}$ indicates the free manifold. The free manifold contains the effects of nonlinearities. The linear operators A and B express the link between Z and S. A expresses the effect of S on Z, while B represents the effect of Z on S. In general, A and B are different. A and B are found by solving the Procrustes minimization problem:

$$A = ZS'(SS')^{-1}, \quad (3)$$

$$B = SZ'(ZZ')^{-1}, \quad (4)$$

Following Navarra and Tribbia (2005), the technique is applied to the principal components of Z and S, therefore the coefficients of the linear operators A and B express the relations between the modes of the two variables. CCA scaling (data scaled by the covariance matrices) is applied to the Principal Components (PCs) of the variables before solving the Procrustes problem:

$$\hat{Z} = (ZZ')^{-1/2}, \quad (5)$$

$$\hat{S} = (SS')^{-1/2}, \quad (6)$$

where $\hat{Z}$ and $\hat{S}$ are the CCA-scaled variables. Please refer to Navarra and Tribbia (2005) for further details of the CM technique.

As explained in Cherchi et al. (2007), after applying the CCA scaling, the elements of A and B are correlation coefficients and can be tested (with a significance test based on the Student t distribution) to reject the null hypothesis of being equal to zero. To improve the robustness of the analysis, each element of the A and B matrices has been verified to be different from zero at the 1% ~~level~~ significance level, following the method proposed by Cherchi et al. (2007).

The CM has two main advantages compared to other methods. The first one is that, when applied to a couple of climate fields (i.e., PRE and SM), CM is able to separate one field (i.e., PRE) into two components: the first component (forced) is the portion of PRE variability that is connected to the SM variability, whereas the second (free) is the part of PRE that is independent from SM. Therefore, the CM technique enables to find robust relations between fields in the presence of strong background noise. The second advantage is that the CM technique is able to detect both local and remote effects of the forcing variable. This is not possible with other methods such as SVD (Singular Value Decomposition).

In the present analysis the CM technique has been applied to the seasonal-mean inter-annual anomalies ~~computed with the data~~. The climatological seasonal cycle has been removed and the data have been stratified using the seasons: JFM (January-February-March), AMJ (April-May-June), JAS (July-August-September) and OND (October-November-December). The JFM, AMJ, JAS, OND stratification has been used by Alessandri and Navarra (2008) in their

CM study of vegetation and rainfall which we will use to compare our results. The trends are kept for their relevance as possible indicators of climate change.

The LAI and SM datasets contain missing values, whose number and position significantly vary with time. The application of the CM algorithms requires that the number and position of the missing values is constant with time. Hence, if a NaN is present in a given grid-point at any time, then it requires to mark as NaN that grid point, thus losing a great amount of information. In order to keep as much information as possible from the data, we decided to replace the missing values with climatological values provided that their total number, considering a particular grid-point, does not exceed a given threshold. We selected different thresholds for SM and LAI in order to obtain as similar as possible spatial coverage of the two variables. The chosen threshold is 10% for LAI and 30% for SM. The results are robust with respect to a ±10% change of the threshold values. As shown in Fig. 1b, the areas more affected by the replacement of SM missing values (30% of values replaced by climatology) are North-East Europe, East coast of Central-South America, East China and Korea. Since the replacement of missing values with climatology reduces time variability, the coupling in these regions may be underestimated as a consequence. We note that these gap-filled regions do not correspond to transition zones between wet and dry climates (Koster et al., 2000). Therefore, they are not expected to display a strong coupling between SM and PRE and to significantly affect the main results of present study.

Since the main interest of the work is on the land-surface, the ocean values are masked out from the PRE dataset. A preliminary analysis (not shown) revealed that their inclusion resulted in a more difficult interpretation of the Empirical Orthogonal Functions (EOF) patterns (Bretherton et al., 1992), due to the interaction of phenomena on different space and time scales which are not connected to land variables.

4 Results

The CM technique has been applied to analyse the reciprocal forcing between PRE and the observed surface variables (SM, ET, LAI). The global-scale reciprocally forced temporal variances between PRE and the land surface variables is reported in Table 2. 19% of the PRE variability is forced by SM. On the other hand, 17% of the SM variance appears to be forced by PRE. 18% of the variability of PRE is forced by ET and 14% of the variance of ET is forced by PRE. Considering the coupling between PRE and LAI, 17% of the variance of PRE

appears to be forced by LAI and 14% of the variability of LAI is forced by PRE. All the variance ratios in Table 2 are significant at the 1% level. The chance of coincidentally getting as high or higher ratios has been tested by means of a Monte Carlo bootstrap method (1000 repetitions).

Since SM is the most important land-surface parameter affecting seasonal to interannual variability/predictability of precipitation (Koster et al., 2000; Zhang et al., 2008), the coupling between SM and PRE will be analyzed in detail in the following.

4.1 Reciprocal forcing between PRE and SM seasonal-mean anomalies

Fig. 2 shows the ratio of the forced/total variance over land. The ratio of SM variance forced by PRE is in panel a, while panel b shows the ratio of PRE variability which is accounted for by the SM variability. For each grid point, the null hypothesis of coincidentally getting as high or higher variance ratios has been tested using a Monte Carlo bootstrap method (1000 repetitions). The regions where the ratio values are not significantly different from zero at the 1% level are dotted. The observed SM variability appears to be intensely forced by PRE over the Sahel and Central-eastern Africa, South Africa, Middle East, the semi-arid region of Central West Asia, Indian Peninsula, Argentina, Eastern Brazil and Australia. Note that, due to the limitations of the satellite estimates discussed in Section 2, large areas in Russia and the Amazon basin are not covered in the SM dataset. The larger observed effects on PRE due to SM inter-annual variability (Fig. 2b) occur in East Brazil, La Plata basin, Sahel, Asian boreal forests, Middle East, Pakistan, Indonesia, northern and eastern Australia. Most of these regions correspond to transition zones between dry and wet climates, where evaporation is highly sensitive to soil moisture (Koster et al., 2000). Here we refer to the transition regions between very dry and very humid environments, as individuated by Koster et al. (2000).

By using the CM technique (described in Section 3), the seasonal-mean PRE anomalies are separated into forced and free components, where forced and free refers to the influence of the SM variation. The variance explained by each mode of the PRE forced field is reported in Table 3. The EOF analysis shows that the first three components of the variability of the forced PRE field together account for 48% of total variance ~~(Table 3)~~. The first two PCs does not display trends while the third PC is dominated by a clear trend, as will be discussed later. The first mode of variability of the forced PRE field explains 26% of the total variance. The corresponding principal component displays two significant peaks at years 1983 and 1992

(Fig. 3a). The PC is significantly correlated (maximum correlation coefficient equal to 0.56 at lag 0) to the stratospheric ~~Aerosol Optical Depth (~~AOD~~), available from the NASA GISS dataset~~. AOD peaks in correspondence of the two major eruptions of the period: 1983 (El Chichon) and 1992 (Pinatubo). The peaks in the AOD time series correspond to those of the forced PRE PC1, suggesting that this mode of variability is related to changes in the solar radiation at the ground, confirming that absorption and reflection of solar radiation by aerosol are particularly effective in reducing the hydrological cycle. The fast response of the precipitation anomalies to the radiation change induced by large tropical volcanic eruptions is in agreement with the results of the lag-correlation analysis by Gu and Adler (2011), who found 0 time lag between stratospheric aerosol signal and PRE. The lagged correlations of PC1 and AOD (Fig. 3b) show that significant (at 5% level) correlations endure up to about 2 years after the aerosol peak (i.e: behind the autocorrelation period of AOD itself; Fig. 3b dashed line). This result indicates that SM may provide a memory of the major volcanic eruptions for PRE. Table 4 shows the variance explained by each EOF mode of the whole original PRE field (that is, forced+free components). The link between PRE and volcanic eruption signal is evident also in the first mode of variability of the total rainfall field as confirmed by the correlation of the corresponding PC (explaining 10% of total PRE variance) with AOD (Table 4).

Fig. 3c shows the ~~horizontal~~ spatial pattern of the first EOF of the PRE anomalies forced by the SM. A clear negative signal is present over areas characterized by a wet climate (Amazon basin, India and Indonesia). In these regions the stratospheric aerosol emitted during the volcanic eruptions has the effect of reducing the intensity of the hydrological cycle (Alessandri et al., 2012) with a consequent reduction of SM, PRE and continental discharge (Trenberth and Dai, 2007). In particular, according to Joseph and Zeng (2011) and Iles et al. (2013), the negative signal over ~~India~~ the monsoon regions may indicate a suppression of the monsoon linked to the effects of the aerosol released during major eruptions ~~according to Iles et al. (2013)~~. Further, differently from our results and other observational (Trenberth and Dai, 2007) and modelling (Joseph and Zeng, 2011) studies, the HadCM3 results of Iles et al. (2013) showed a wetting signal over India during the summer season (although not significant in the observational dataset they used). On the other hand, over transition zones (U.S. Great Plains, Argentina, Middle East) the dimming effect may result in reduced evapotranspiration during the hot/dry season which drives an increase of SM (Wild et al., 2009). During the following cool/wet season, the enhanced SM can induce a lagged increase of the portion of

PRE forced by SM. That can explain the increased PRE over transition areas. On the other hand, the reduction of PRE over South Asia monsoon region and the enhancement of PRE over the semi-arid areas of Central West Asia is consistent with the monsoon-desert mechanism (Rodwell and Hoskins, 1996; Cherchi et al., 2014): the reduction of radiation caused by the stratospheric aerosol drives a reduction of convection over monsoon regions and a consequent reduction of PRE over South Asia therefore abating Rossby wave induced subsidence over Middle East and East Mediterranean (Cherchi et al., 2014).

The second PC of PRE forced by SM, explaining 14% of total variance, is dominated by a large scale oscillation (Fig. 4a). The corresponding principal component (full line) displays an high correlation coefficient of 0.60 with the NINO3 index (average of the Sea Surface Temperature in the tropical Pacific region 5S–5N, 210–270E; dashed line) at lag 2 (significant at the 1% level), indicating that EOF2 represents the portion of the rainfall forced by SM that is related to the El Niño Southern Oscillation (ENSO; Philander, 1989) variability. ~~The HadISST 1.1 – Global sea-Ice coverage and Sea Surface Temperature (1870-Present; Rayner et al., 2003) dataset has been used to compute the NINO3 index.~~ The second mode of forced PRE response due to SM variability appears to be lagged by one to several seasons with respect to the ENSO phase (Fig. 4b), with the strongest correlations with the NINO3 index two seasons after the maximum El Niño or La Niña intensity and significant correlations enduring until the lag 5 season (i.e: behind the autocorrelation period of ENSO itself; Fig. 5b dashed line). The results indicate that the effects related to ENSO in the SM may induce a delayed forcing on PRE. Therefore, SM appears to provide a biophysical memory of ENSO on the global precipitation pattern. The signal of ENSO can also be evidenced in the second mode of variability of the total rainfall field as indicated by the correlation of the corresponding PC (explaining 5% of total PRE variance) with NINO3 (Table 4). Again, the lag at which maximum correlation is attained is the same (lag 2) as in the forced field but the correlation coefficient is 0.60 for the forced field and 0.43 for the total PRE field.

The ~~horizontal~~ spatial pattern of the second EOF of the PRE anomalies forced by SM (Fig. 4c) displays the signature of the tripole pattern over south America typical of ENSO teleconnections (Ropelewski and Halpert, 1989). Similarly, negative PRE anomalies are shown over Brazil, South Africa, North India and Indochina, displaying the land surface feedback to the reduced rainfall related to the positive phase of ENSO there (Trenberth et al., 1998). On the other hand, positive precipitation anomalies characterize the West and East

Coasts of North America, Central America, the dry and semi-arid region of North Venezuela, La Plata basin, Horn of Africa, Sahel, Europe, Central and East Asia, South India and the East Coast of Australia. Most previous research showed reduced precipitation over India during ENSO years (Ropelewski and Halpert, 1989; Trenberth et al., 1998). The positive anomalies of PRE forced by SM over South India related to the positive phase of ENSO evidence an interesting negative feedback of the land-surface on the effect of ENSO on the rainfall over India.

The third PC of the PRE forced by the SM, explaining 8% of forced variance, displays a trend (Fig. 5a) corresponding to a clear signal of increasing precipitation over the Sahel, South-East Europe, Central Asia, North-East Asia, the Great Plains of North America, Nordeste and the Northern part of South America (Fig. 5b). The trend of increasing precipitation is particularly strong over the Sahel where, according to Hagos and Cook (2008), it can be related to a warming of the northern tropical Atlantic Ocean which, through a modification of the associated cyclonic circulation, enhances moisture transport over the region. In contrast, a decrease of precipitation is evident over most of the Southern Hemisphere (SH), North West Russia, East Russia, North India, China and West US, showing a north-south polarity of the precipitation trend. The above trend pattern strongly resembles the trend pattern of global rainfall annual mean anomalies described by Munemoto and Tachibana (2012, hereinafter MT12). The authors associated this North-South polarity to a relatively larger warming of the Northern Hemisphere (NH) compared to the SH that characterized the last three decades starting from the early 1980s. MT12 found that the trend of the SST corresponds to an increase of the specific humidity in the NH with respect to SH that enhances (reduces) precipitation in the NH (SH). Although the focus of MT12 is on the Sahel region, the authors defined a global index, the North South SST (NS-SST) polarity index, which successfully captures the global signal of the precipitation trend. The NS-SST index is defined as the area averaged NH SST annual mean anomalies minus the SH SST anomalies. The NS-SST index (computed from HadISST), normalized by its standard deviation, and its trend are plotted in Fig. 5a. Note that here the NS-SST index is computed from the seasonal mean anomalies instead of the annual mean anomalies used in MT12, nonetheless the trend is not affected.

4.2 Mediation effects of ET and LAI on the coupling between PRE and SM

To investigate how the coupling between rainfall and soil moisture is mediated by evapotranspiration and vegetation we further applied the CM technique between the

component of PRE forced by SM and ET (LAI), obtaining the component of PRE forced by SM which is also forced by ET (LAI). As summarized in Table 5, 20% of the inter-annual variability of the PRE anomalies forced by the SM is estimated to be globally forced by the ET variation. It is important to note here that 19%x20%=3.8% represents only the ET forcing on PRE mediated by SM and not the whole ET forcing on PRE which is actually 18% (Table 2). At the same time, 23% of the variance of PRE forced by SM is evaluated to be also forced by LAI, therefore the LAI forcing on PRE mediated by SM corresponds to 17%x23%=3.9%.

Fig. 6a shows the ratio of the variance of PRE forced by the SM which is also forced by the ET with respect to the total forced rainfall variance. Fig. 6b shows the same plot but for the LAI. The "hotspots" in Fig. 6a are similar to those found in Fig. 2b over Sahel, Horn of Africa, East Europe, Asian boreal forests, Central Asia, West Coast of the US, East Brazil and La Plata basin. This indicates that in all these regions the link between PRE and SM is at least in part mediated by ET. Not surprisingly, the same regions also display a link with vegetation (Fig. 6b). Furthermore, vegetation appears to significantly affect rainfall variability over the semi-arid regions that are not dependent on ET such as Central West Asia, South-East Africa, South-East Asia and West Australia, suggesting that in these regions the SM forcing on PRE is mediated by vegetation state (e.g. stress of vegetation will affect PRE there).

To analyse how the response of PRE forced by SM to climate events and the trend are mediated by ET (LAI), we applied the CM technique between each of the physical fields corresponding to the first three modes of variability of PRE forced by the SM and ET (LAI). Here we take the physical fields corresponding to the first three modes of variability of PRE forced by SM and further decompose them to extract the parts of each mode that is forced by ET and LAI, respectively. This analysis allows to figure out how ET and LAI contribute to each component of PRE forced by SM which has been identified to be linked to external climate forcing (volcanic eruptions, ENSO and trend). Overall, considering the global land, 21% of the variance displayed by the first mode (linked to volcanic eruptions) of PRE forced by the SM is forced by the ET and 27% by LAI (Table 6). As for the second mode (connected to ENSO), 38% of the variance is forced by ET and 36% by LAI. Concerning the third mode (displaying a trend), 31% of the variance is forced by ET and 29% is forced by LAI. Rainfall variability forced by the ET and LAI decomposed through EOF analysis is reported in Table 7. Interestingly, the third PC of the PRE forced by the ET (explaining 7% of the forced variance) is correlated with AOD, with a maximum correlation coefficient of 0.41 at lag 6.

Analogously, the second PC of the PRE anomalies forced by the LAI (explaining 10% of the forced variance) is correlated with AOD, with a maximum correlation coefficient of 0.41 at lag 3, suggesting that both ET and vegetation contribute to provide memory of volcanic eruptions, modulating at longer scales the effect of the SM forcing on PRE. The first PC of PRE forced by ET (explaining 30% of the forced variance) is found to be significantly correlated with the NINO3 index with a correlation coefficient of 0.52 at lag 0. The first PC of PRE forced by LAI (explaining 27% of the forced variance) also has a maximum correlation coefficient of 0.67 at lag 0 with the NINO3 index, indicating that vegetation acts as the mediator at longer scales of the signal between SM and PRE. This result is consistent with the relationship found by Alessandri and Navarra (2008) between precipitation forced by vegetation (NDVI) and ENSO and with the delayed vegetation response to ENSO signal found by Zeng et al. (2005). All the above correlation coefficients passed a significance test at 1% level.

To determine the regions where the mediating effects of ET and LAI have the larger influence on the coupling with respect to the stratospheric volcanic eruptions, the first mode of variability of PRE forced by the SM has been correlated with the total components of PRE forced by the ET and LAI. The correlation coefficients are shown in Fig. 7a for PRE forced by the ET and Fig. 7b for PRE forced by the LAI. Only the regions where correlations passed a significance test at 5% level are shaded. Black upward (white downward) triangles denote areas with positive (negative) values of the first EOF of the PRE anomalies forced by the SM (Fig. 3c). The correlations are positive almost everywhere (i.e. the effects of both ET and LAI tend to amplify the response of rainfall to large volcanic eruptions) and the patterns are very similar for ET and LAI, indicating that the feedback of ET may be linked to the stress of vegetation consequent to the effect of volcanic eruptions on radiative forcing. Large values (up to 0.6) are seen over Central US, North West Brazil, La Plata basin, West Central Asia, Horn of Africa, South Africa, the Asian monsoon region, Indonesia and Australia. Over these regions evapotranspiration and vegetation activity are radiation limited (Seneviratne et al., 2010). Nevertheless, while over some regions (Southern part of North America, La Plata basin, Middle East, West Central Asia and Horn of Africa) ET and LAI contribute to an increase of rainfall, over other regions (Norther South America, South Africa, Indian monsoon region, Australia) they contribute to rainfall reduction. As discussed in Section 4.1, over most of the SH (apart from La Plata basin and Horn of Africa) and the Asian monsoon region there is a reduction of precipitation that can be associated to the dimming effect and

the consequent reduction of the hydrological cycle. In humid regions the rainfall reduction can stress vegetation and may reduce its growth with effects lasting up to one year (Wang et al., 2011b). On the other hand, over most of the arid and semi-arid regions (Middle East, West Central Asia), the reduced evapotranspiration during past seasons induced by the dimming effect may increase SM and therefore attenuate the stress on vegetation. This, in turn, has a positive effect on precipitation.

The point-by-point correlation coefficient between the second mode of variability (related to ENSO) of PRE forced by the SM and the total fields of PRE forced by the ET and PRE forced by the LAI is shown in Fig. 8 on panel a and b, respectively. The sign of the feedback between PRE and SM is indicated by the second EOF of PRE forced by the SM overlaid to the plot. Large positive correlations up to 0.6 are found globally over most of the land areas. ET has a positive feedback on the increase of precipitation over the West Coast of US, the dry and semi-arid region of North Venezuela, La Plata basin, Sahel, North Europe, India, Central and East Asia and the South-East Coast of Australia. Still a positive feedback is present over Brazil, South Africa and Indochina but in this case ET leads to further reduction of PRE. A negative feedback of ET is seen over Mexico. In this region the positive ENSO phase induces wet and cool conditions (Trenberth et al., 1998) associated to an increase of PRE forced by SM that is contrasted by a reduction of ET. As for vegetation, it contributes to rainfall enhancement over East and West Coasts of the US, La Plata basin, North Europe, Horn of Africa, the semi-arid region of West Central Asia and East Asia. Conversely, vegetation mediates precipitation reduction over Brazil, South Africa and Indochina.

Fig. 9 shows the point-by-point correlation coefficient between the third mode of variability of PRE forced by the SM (displaying a linear trend, see Fig. 5) and the total fields of PRE forced by the ET (Fig. 9a) and PRE forced by the LAI (Fig. 9b) with the third EOF of PRE forced by the SM overlaid on it. The feedback of ET on this mode of variability of PRE is not significant over most of the NH. A positive effect of ET is seen over the semi-arid regions of the SH but while over Sahel ET mediates an increase of rainfall, over Bolivia and Australia ET leads to further reduction of PRE (Fig. 9a). On the other hand, ET has a negative feedback over the humid region of Tanzania where it contrasts the reduction of PRE. The pattern of the feedback of LAI (Fig. 9b) is very different from that of ET. Overall, the vegetation has a positive feedback on the rainfall anomaly pattern forced by the SM. In particular, large correlations up to 0.6 are seen over the Sahel, East Coast of the US, West South America,

East Europe, Tropical South Africa, West Central Asia, Asian boreal forests, Central and East Asia, the Indian monsoon region and East Australia. The strong signal over the Sahel is in agreement with Zeng et al. (1999) and Kucharski et al. (2013) who found that vegetation feedback amplifies rainfall response to the SST variations on the decadal scale. LAI mediates rainfall enhancement over the Sahel, East Coast of the US, Europe, the semi-arid region of West Central Asia and the Indian monsoon region. Conversely, vegetation contributes to a reduction of PRE over most of the SH (in particular over South America, South Africa and East Australia), the West Coast of the US and East Asia. Fig. 9c shows the linear vegetation trend over the period 1982-2010. Only areas where trend passed a significance test at the 5% level are shown. Significant positive (greening) trend is seen in large parts of the NH (the East Coast of the US, Sahel, Europe, West Central Asia, India and Asian boreal forests). A negative vegetation trend (browning) appears over the West Coast of the US, West South America, the tropical region of South Africa and East Asia. The greening/browning trends in Fig. 9c are consistent with those found by de Jong et al. (2013). A comparison of panels b and c of Fig. 9 evidences that most of the areas characterized by a positive trend of rainfall anomalies are associated to a greening trend of vegetation while areas displaying a decrease of PRE are regions associated to a browning trend. Therefore, the response of rainfall anomalies forced by the SM to the inter-hemispheric SST trend appears to be coupled to a greening/browning trend of vegetation activity. Furthermore, the third PC of PRE forced by LAI displays a trend similar to that of the NS-SST index, analogously to the third PC of PRE forced by SM, while no trends are found in the first five PCs of PRE forced by ET.

5 Conclusions

A global array of relevant up-to-date ~~state-of-the-art~~high quality datasets (soil moisture, evapotranspiration, leaf area index and precipitation) is acquired, harmonized and analysed. For the first time a long comprehensive global observational dataset is used to characterize the land variability as a function of the space and time scales and to improve understanding of the relationships and feedbacks between land and climate. By applying the Coupled Manifold technique on the seasonal-mean inter-annual anomalies, the relationship and the coupling between the acquired surface variables is assessed considering all the seasons.

The analysis shows a considerable degree of reciprocal forcing and coupling in the land surface variables considered. The reciprocal forcing with precipitation is particularly strong

for the soil moisture, with 19% of the inter-annual variability of the precipitation over continental areas that are forced by the SM variation. Conversely, 17% of the SM variance is forced by PRE.

The PRE forced by the SM is dominated by a prominent decadal-scale drying, initiated by the perturbation of the abrupt Mt. Pinatubo eruption. In 1991, the PC1 of the dominant forced mode of PRE shows an abrupt decrease and the negative anomaly continues increasing in the subsequent years until 1994. It is only after 1995 that the rainfall starts to slowly recover towards the pre-eruption levels. In 1997, the signal sums-up with that of ENSO. It appears that the persistence of the negative SM anomalies leads to increasing stress conditions for the vegetation, thus leading to a larger ET response at longer time-lags after the perturbing event. Our interpretation is that the persistence of the negative SM anomalies provides the memory of the initial perturbing event and our analysis indicate that, through this mechanism, the effect of Mt. Pinatubo eruption can last for several years and its memory appears to extend and sum to the following 1997-1998 El Niño event. The second PC of the PRE forced by the SM displays a large-scale oscillation correlated to ENSO variability with significant correlations enduring behind the autocorrelation period of ENSO itself and up to more than one year lag. This indicates that ENSO effects on SM induce a delayed forcing on PRE. The third PC of the PRE forced by the SM is dominated by a trend, positive over most of the NH and negative over most of the SH. This trend appears to be related to the inter-hemispheric SST contrast to which corresponds an increase of the specific humidity in the NH with respect to the SH that enhances (reduces) precipitation and SM in the NH (SH).

The combined analysis of the PRE modes related to the external climate forcings (volcanic eruptions, ENSO, SST trend) and the rainfall forced by ET and LAI evidences the role of ET and LAI as the mediators between SM forcing and rainfall. In particular, it appears that both ET and LAI tend to provide a positive feedback on PRE over most of the regions, contributing to further enhance or reduce rainfall depending on the regions of the globe, with large differences between wet, transition and semi-arid climates. Nevertheless, the response to ENSO is characterized by a negative feedback of ET over regions where the positive ENSO phase induces wet and cool conditions (i.e. Mexico).

It is important to note that the coupling with SM revealed by the present analysis has to be considered an underestimation of the real coupling, due to the incomplete cover of the SM

dataset. Nevertheless, the present investigation identifies the regions characterized by a strong coupling and suggests most possible mechanisms linking the considered variables.

Since SM has been recognized as the most important land-surface parameter affecting seasonal to interannual variability of precipitation (Koster et al., 2000; Zhang et al., 2008) the present paper focused on the coupling between SM and PRE. Detailed analysis of the reciprocal forcing between ET and LAI, LAI and SM and ET and SM will be the subject a future paper that will further address the specific coupling among land-surface variables.

Data availability

Evapotranspiration dataset available from the Numerical Terradynamic Simulation Group (NTSG) of the University of Montana. Web: http://www.ntsg.umt.edu/project/et

Leaf Area Index dataset available from the Department of Earth & Environment of Boston University. Web: http://sites.bu.edu/cliveg/datacodes/

Soil Moisture dataset available from the European Space Agency (ESA) Climate Change Initiative (CCI). Web: http://www.esa-soilmoisture-cci.org/

Precipitation dataset available from the Global Precipitation Climatology Project (GPCP). Web: http://precip.gsfc.nasa.gov/

Aerosol Optical Depth dataset available from the National Aeronautics and Space Administration (NASA) Goddard Institute for Space Studies (GISS). Web: http://data.giss.nasa.gov/modelforce/strataer/

Sea Surface Temperature dataset available from the Hadley Centre for Climate Prediction and Research (2006): Met Office HadISST 1.1 (Global sea-Ice coverage and Sea Surface Temperature). Web: http://catalogue.ceda.ac.uk/uuid/facafa2ae494597166217a9121a62d3c

Acknowledgements

The research leading to these results has received funding from the European Union Seventh Framework Programme (FP7/2007- 2013) under SPECS project (grant agreement n° 308378) and by the LIFE10 ENV/FR/208 project FO3REST. We are grateful to the two anonymous reviewers whose comments greatly improved the quality of the manuscript.

References

Adler, R. F., and Coauthors: The Version-2 Global Precipitation Climatology Project (GPCP) Monthly Precipitation Analysis (1979–Present), J. Hydrometeorol., 4, 1147-1167, 2003.

Alessandri, A., and Navarra, A.: On the coupling between vegetation and rainfall inter-annual anomalies: Possible contributions to seasonal rainfall predictability over land areas, Geophys. Res. Lett., 35, L02718., 2008.

Alessandri, A., and Coauthors: The INGV-CMCC Seasonal Prediction System: Improved Ocean Initial Conditions Mon. Weather Rev. 138 (7), 2930-2952, 2010.

Alessandri, A., Borrelli, A., Navarra, A., Arribas, A., Déqué, M., Rogel, P., and Weisheimer, A.: Evaluation of probabilistic quality and value of the ENSEMBLES multi-model seasonal forecasts: comparison with DEMETER. Mon. Weather Rev., 139 (2), 581-607, doi:10.1175/2010MWR3417.1, 2011.

Alessandri, A., Fogli, P. G., Vichi, M., and Zeng, N.: Strengthening of the hydrological cycle in future scenarios: atmospheric energy and water balance perspective. Earth Syst. Dynam. 3, 199-212, 2012.

Bretherton, C. S., Smith, C., and Wallace, J. M.: An intercomparison of methods for finding coupled patterns in climate data. J. Climate, 5, 541-560, 1992.

Cherchi, A., Gualdi, S., Behera, S., Luo, J. J., Masson, S., Yamagata, T., and Navarra, A.: The influence of tropical indian ocean SST on the indian summer monsoon, J. Clim., 20, 3083-3105, 2007.

Cherchi, A., Annamalai, H., Masina, S., and Navarra, A.: South Asian Summer Monsoon and the Eastern Mediterranean Climate: The Monsoon–Desert Mechanism in CMIP5 Simulations, J. Clim., 27, 6877-6903, 2014.

De Felice, M., Alessandri, A., and Catalano, F.: Seasonal climate forecasts for medium-term electricity demand forecasting, Appl. Energy, 137, 435-444, 2014.

de Jong, R., Verbesselt, J., Zeileis, A., and Schaepman, M. E.: Shifts in Global Vegetation Activity Trends, Remote Sens., 5, 1117-1133, 2013.

Dirmeyer, P. A.: The terrestrial segment of soil moisture–climate coupling, Geophys. Res. Lett., 38, L16702., 2011.

Ferranti, L., and Viterbo, P.: The European summer of 2003: Sensitivity to soil water initial conditions, J. Clim., 19, 3659–3680, 2006.

Gu, G., and Adler, R. F.: Precipitation and Temperature Variations on the Interannual Time Scale: Assessing the Impact of ENSO and Volcanic Eruptions, J. Clim., 24, 2258–2270, 2011.

Hagos, S. M.., and Cook, K. H.: Ocean Warming and Late-Twentieth-Century Sahel Drought and Recovery, J. Clim., 21, 3797–3814, 2008.

Hohenegger, C., Brockhaus, P., Bretherton, C. S., and Schar, C.: The Soil Moisture–Precipitation Feedback in Simulations with Explicit and Parameterized Convection, J. Clim., 22, 5003–5020, 2009.

Iles, C. E., Hegerl, G. C., Schurer, A. P., and Zhang, X.: The effect of volcanic eruptions on global precipitation, J. Geophys. Res. Atmos., 118, 8770–8786, doi:10.1002/jgrd.50678, 2013.

Joseph, R., and Zeng, N.: Seasonally modulated tropical drought induced by volcanic aerosol, J. Clim., 24(8), 2,045–2,060, doi:10.1175/2009JCLI3170.1, 2011.

Koster, R. D., Suarez, M. J., and Heiser, M.: Variance and predictability of precipitation at seasonal-to-interannual timescales, J. Hydrometeor., 1, 26-46, 2000.

Koster, R. D., and Coauthors: Regions of Strong Coupling Between Soil Moisture and Precipitation. Science, 305, 338-340, 2004.

Koster, R. D., Guo, Z., Yang, R., Dirmeyer, P. A., Mitchell, K., and Puma, M. J.: On the Nature of Soil Moisture in Land Surface Models, J. Clim., 22, 4322-4335, 2009.

Kucharski, F., Zeng, N, and Kalnay, E.: A further assessment of vegetation feedback on decadal Sahel rainfall variability, Climate Dyn., 40, 1453-1466, DOI:10.1007/s00382-012-1397-x, 2013.

Liu, Y. Y., Parinussa, R. M., Dorigo, W. A., De Jeu, R. A. M., Wagner, W., van Dijk, A. I. J. M., McCabe, M. F., and Evans, J. P.: Developing an improved soil moisture dataset by blending passive and active microwave satellite based retrievals. Hydrology and Earth System Sciences, 15, 425–436, 2011.

Liu, Y. Y., Dorigo, W. A., Parinussa, R. M., De Jeu, R. A. M., Wagner, W., McCabe, M. F., Evans, J. P., van Dijk, A. I. J. M.: Trend-preserving blending of passive and active microwave soil moisture retrievals. Remote Sens. Env., 123, 280–297, 2012.

Navarra, A., and Tribbia, J.: The coupled manifold, J. Atmos. Sci., 62, 310-330, 2005.

Pal, J. S., and Eltahir, E. A. B.: A feedback mechanism between soil-moisture distribution and storm tracks, Q. J. R. Meteorol. Soc., 129, 2279-2297, 2003.

Philander, S.G.H.: El Niño, La Niña and the Southern Oscillation. Academic Press, New York, 293 pp, 1989.

Rayner, N. A., Parker, D. E., Horton, E. B., Folland, C. K., Alexander, L. V., Rowell, D. P., Kent, E. C., and Kaplan, A.: Global analyses of sea surface temperature, sea ice, and night marine air temperature since the late nineteenth century, J. Geophys. Res., Vol. 108, No. D14, 4407 10.1029/2002JD002670, 2003.

Rodwell, M. J., and Hoskins, B. J.: Monsoons and the dynamics of deserts, Q. J. R. Meteorol. Soc., 122, 1385-1404, 1996.

Ropelewski, C. F., and Halpert, M. S.: Precipitation Patterns Associated with the High Index Phase of the Southern Oscillation, J. Clim., 2, 268–284, 1989.

Rosati, A., Miyakoda, K., and Gudgel, R.: The impact of ocean initial conditions on ENSO forecasting with a coupled model. Mon. Wea. Rev., 125, 754–772, 1997.

Santanello, J. A., Peters-Lidard, C. D., Kumar, S. V., Alonge, C., and Tao, W.-K.: A Modeling and Observational Framework for Diagnosing Local Land-Atmosphere Coupling on Diurnal Time Scales, J. Hydrometeor., 10, 577-599, 2009.

Sato, M., Hansen, J. E., McCormick, M. P., and Pollack, J. B.: Stratospheric aerosol optical depth, 1850-1990. J. Geophys. Res. 98, 22987-22994, 1993.

Self, S., Rampino, M. R, Zhao, J., and Katz, M. G.: Volcanic aerosol perturbations and strong El Nino events: No general correlation. Geophys. Res. Lett., 24, 1247−1250, 1997.

Seneviratne, S. I., Corti, T., Davin, E. L., Hirschi, M, Jaeger, E. B., Lehner, I., Orlowsky, B., and Teuling, A. J.: Investigating soil moisture–climate interactions in a changing climate: A review. Earth Sci. Rev., 99, 125−161, 2010.

Shukla, J., and Kinter, J. C.: Predictability of seasonal climate variations: A pedagogical review. Predictability of Weather and Climate, T. Palmer and R. Hagedorn, Eds., Cambridge University Press, 306–341, 2006.

Trenberth, K. E., Branstator, G. W., Karoly, D., Kumar, A., Lau, N.-C., and Ropelewski, C.: Progress during TOGA in understanding and modelling global teleconnections associated with tropical sea surface temperatures. J. Geophys. Res., 103, 14,291-14,324, 1998.

Trenberth, K. E., and Dai, A.: Effects of Mount Pinatubo volcanic eruption on the hydrological cycle as an analog of geoengineering. Geophys. Res. Lett., 34, L15702, 2007.

Wang, B., and Coauthors: Advance and prospectus of seasonal prediction: Assessment of the APCC/CliPAS 14-model ensemble retrospective seasonal prediction (1980–2004). Climate Dyn., 33, 93–117, 2009.

Wang, G., Dolman, A. J., and Alessandri, A.: A summer climate regime over Europe modulated by the North Atlantic Oscillation, Hydrol. Earth Syst. Sci., 15, 57-64, 2011a.

Wang, G., Sun, S., and Mei, R.: Vegetation dynamics contributes to the multi-decadal variability of precipitation in the Amazon region, Geophys. Res. Lett., 38, L19703, 2011b.

Wild, M., Trüssel, B., Ohmura, A., Long, C. N., König-Langlo, G., Dutton, E. G., and Tsvetkov, A.: Global dimming and brightening: An update beyond 2000, J. Geophys. Res., 114, D00D13, doi:10.1029/2008JD011382, 2009.

Zeng, F.-W., Collatz, G. J., Pinzon, J. E., and Ivanoff, A.: Evaluating and Quantifying the Climate-Driven Interannual Variability in Global Inventory Modeling and Mapping Studies (GIMMS) Normalized Difference Vegetation Index (NDVI3g) at Global Scales, Remote Sens., 5, 3918-3950, 2013.

Zeng, N., Neelin, J., Lau, W.-M., and Tucker, C.: Enhancement of interdecadal climate variability in the Sahel by vegetation interaction, Science, 286, 1537–1540, 1999.

Zeng, N., Mariotti, A., and Wetzel, P.: Terrestrial mechanisms of interannual CO2 variability, Global Biogeochem. Cycles, 19, GB1016, doi:10.1029/2004GB002273, 2005.

Zhang, K., Kimball, J. S., Nemani, R. R., and Running, S. W.: A continuous satellite-derived global record of land surface evapotranspiration from 1983 to 2006, Water Resour. Res., 46, W09522, doi:10.1029/2009WR008800, 2010.

Zhang, J., Wang, W.-C., and Wei, J.: Assessing land-atmosphere coupling using soil moisture from the Global Land Data Assimilation System and observational precipitation, J. Geophys. Res., Vol. 113, No. D17119, doi:10.1029/2008JD009807, 2008.

Zhu, Z., Bi, J., Pan, Y., Ganguly, S., Anav, A., Xu, L., Samanta, A., Piao, S., Nemani, R. R., and Myneni, R. B.: Global Data Sets of Vegetation Leaf Area Index (LAI)3g and Fraction of Photosynthetically Active Radiation (FPAR)3g Derived from Global Inventory Modeling and Mapping Studies (GIMMS) Normalized Difference Vegetation Index (NDVI3g) for the Period 1981 to 2011, Remote Sens., 5, 927-948, 2013.

Table 1. Evapotranspiration (ET) [Zhang et al., 2010], Leaf Area Index (LAI) [Zhu et al., 2013], Soil Moisture (SM) [Liu et al., 2011, 2012], Precipitation (PRE) [Adler et al., 2003] ~~D~~datasets characteristics.

	ET	LAI	SM	PRE
type	satellite	satellite	satellite	gridded from rain gauges
version	-	1.0	0.1	2.2
producer	University of Montana	Boston University	ESA	GPCP
Spatial resolution (original)	1° x 1°	8 km x 8 km	0.25° x 0.25°	2.5° x 2.5°
Spatial resolution (after pre-processing)	1° x 1°	0.5° x 0.5°	0.5° x 0.5°	2.5° x 2.5°
Temporal frequency (original)	monthly	15-days	daily	monthly
Temporal frequency (after pre-processing)	seasonal	seasonal	seasonal	seasonal
units	$W\ m^{-2}$	$m^2\ m^{-2}$	$m^3\ m^{-3}$	$mm\ d^{-1}$
period	1983-2006	1982-2010	1979-2010	1979-2010

Table 2. Ratios of the global-scale forced and free variance with respect to the total variance resulting from the application of the CM technique between PRE and SM, ET and LAI.

	Forced	Free
SM	0.17	0.83
PRE	0.19	0.81
ET	0.14	0.86
PRE	0.18	0.82
LAI	0.14	0.86
PRE	0.17	0.83

Table 3. ~~Rainfall~~ PRE variability forced by the SM decomposed through EOF analysis. Each line displays the EOF explained variance (column 2) and the corresponding PC correlation with relevant climatic indices (column 3). AOD is the Stratospheric Aerosol Optical Depth. NINO3 index is defined as the average of the Sea Surface Temperature in the tropical Pacific region (5◦ S–5◦ N, 210–270◦ E). Here the maximum PC correlation is reported considering lagged correlations in the range -16 to +16. Only the correlation coefficients significant at 1% level are reported.

	Variance explained	Correlation with climate indices
PC 1	0.26	0.56 (AOD) at lag 0 (significant in the range: -4/+7)
PC 2	0.14	0.60 (NINO3) at lag 2 (significant in the range: 0/+5)
PC 3	0.08	-
PC >4	<0.07	-

Table 4. Total rainfall variability decomposed through EOF analysis. Each line displays the EOF explained variance (column 2) and the corresponding PC correlation with relevant climatic indices (column 3). Here the maximum PC correlation is reported considering lagged correlations in the range -16 to +16. Only the correlation coefficients significant at 1% level are reported.

	Variance explained	Correlation with climate indices
PC 1	0.10	0.41 (AOD) at lag 0 (significant in the range: -2/+2)
PC 2	0.05	0.43 (NINO3) at lag 2 (significant in the range: +1/+4)
PC >3	<0.04	-

Table 5. Ratios of the global-scale forced and free variance with respect to the total variance resulting from the application of the CM technique between PRE forced by SM and ET, LAI.

	Forced	Free
PRE forced by SM (forced by ET)	0.20	0.80
PRE forced by SM (forced by LAI)	0.23	0.77

Table 6. Ratios of the global-scale forced variance over the total variance resulting from the application of the CM technique between the first three modes of PRE forced by SM and the total fields of ET and LAI.

	ET	LAI
PRE forced by SM mode 1	0.21	0.27
PRE forced by SM mode 2	0.38	0.36
PRE forced by SM mode 3	0.31	0.29

Table 7. Rainfall variability forced by the ET and LAI decomposed through EOF analysis. Each line displays the EOF explained variance (column 2) and the corresponding PC correlation with relevant climatic indices (column 3). Here the maximum PC correlation is reported considering lagged correlations in the range -16 to +16. Only the correlation coefficients significant at 1% level are reported.

	Variance explained	Correlation with climate indices
PRE forced by ET		
PC 1	0.30	0.52 (NINO3) at lag 0 (significant in the range: -2/+2)
PC 2	0.13	-
PC 3	0.07	0.41 (AOD) at lag 6 (significant in the range: +3/+10)
PC >4	<0.05	-
PRE forced by LAI		
PC 1	0.27	0.67 (NINO3) at lag 0 (significant in the range: -2/+2)
PC 2	0.10	0.41 (AOD) at lag 3 (significant in the range: 0/+5)
PC 3	0.09	-
PC >4	<0.06	-

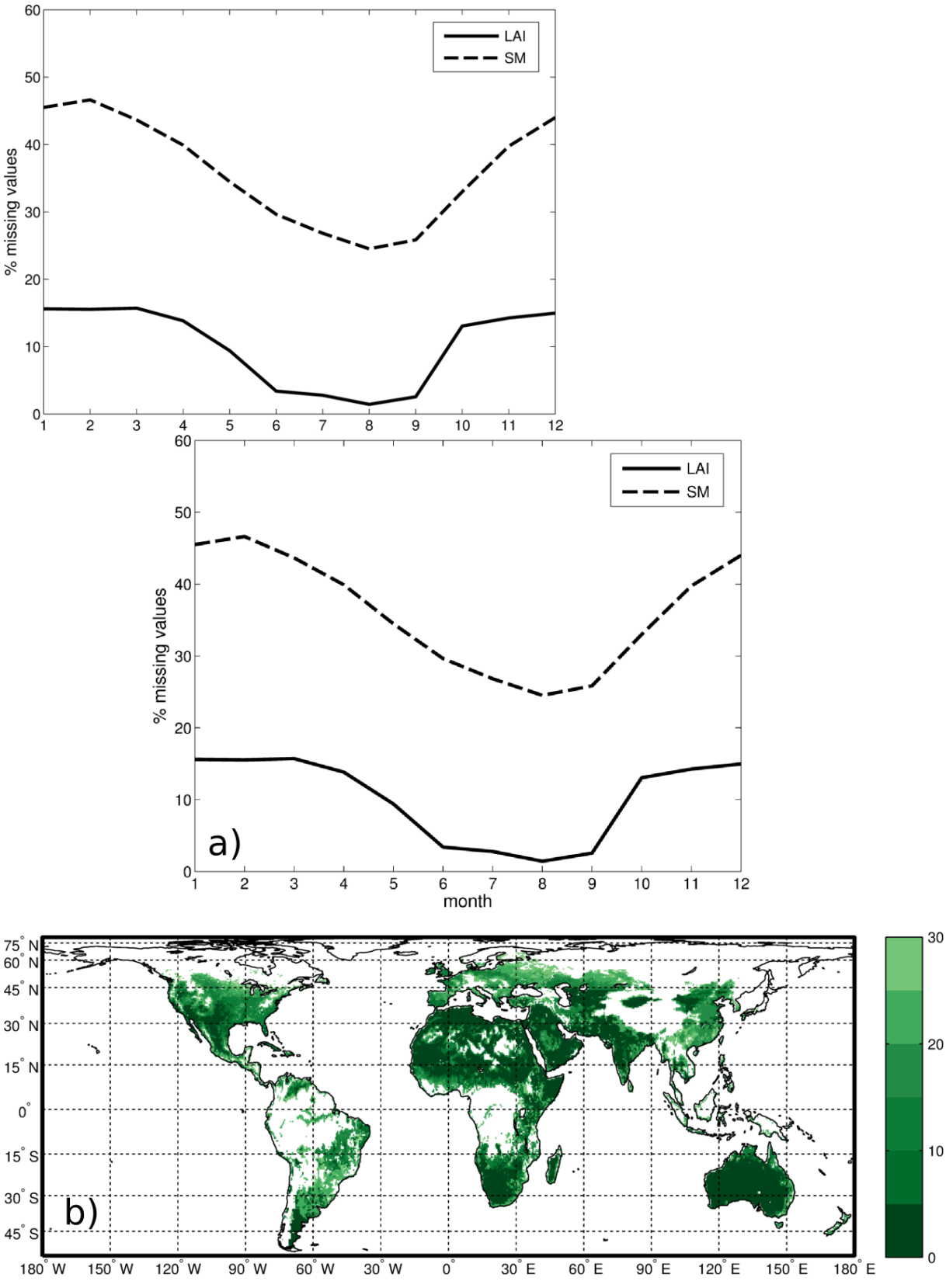
LAI
SM
% missing values
month
a)
b)
75° N
60° N
45° N
30° N
15° N
0°
15° S
30° S
45° S
180° W
150° W
120° W
90° W
60° W
30° W
0°
30° E
60° E
90° E
120° E
150° E
180° E
30
20
10
0

Figure 1. (a) Global mean missing values in the time series (in %): LAI (full), SM (dashed). (b) Map of the percentage of SM missing data for each grid point.

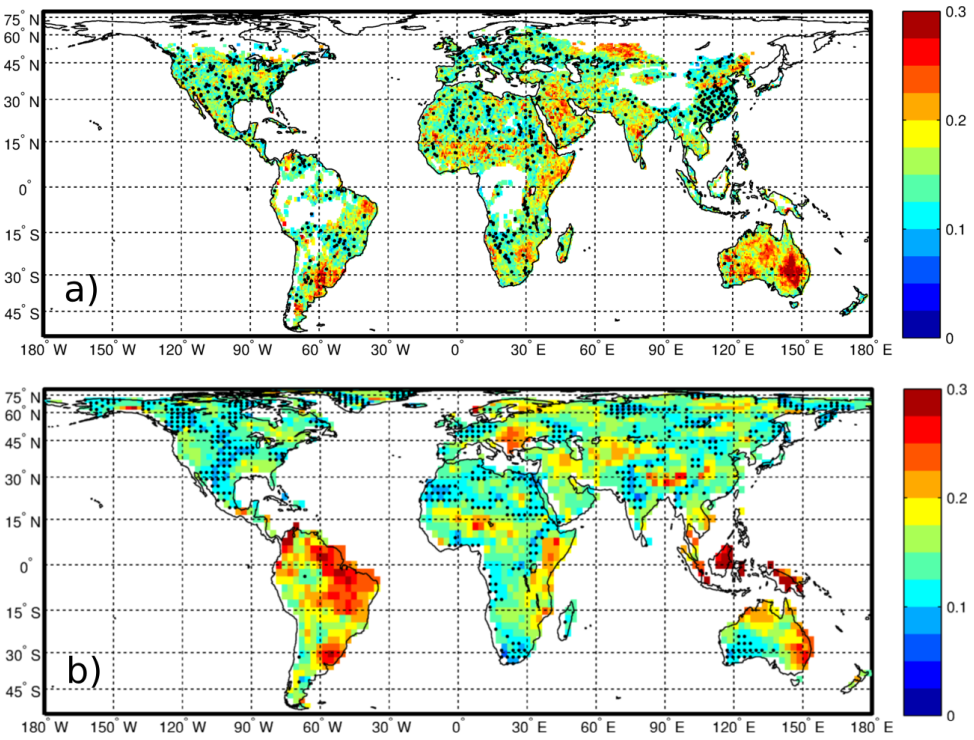

Figure 2. Ratio of the forced variance to the total variance. (a) The fraction of SM variance forced by PRE. (b) The fraction of PRE variance forced by the SM. Dots are placed over areas covered by the forced variable dataset but where variance ratio values did not pass a significance test at the 1% level.

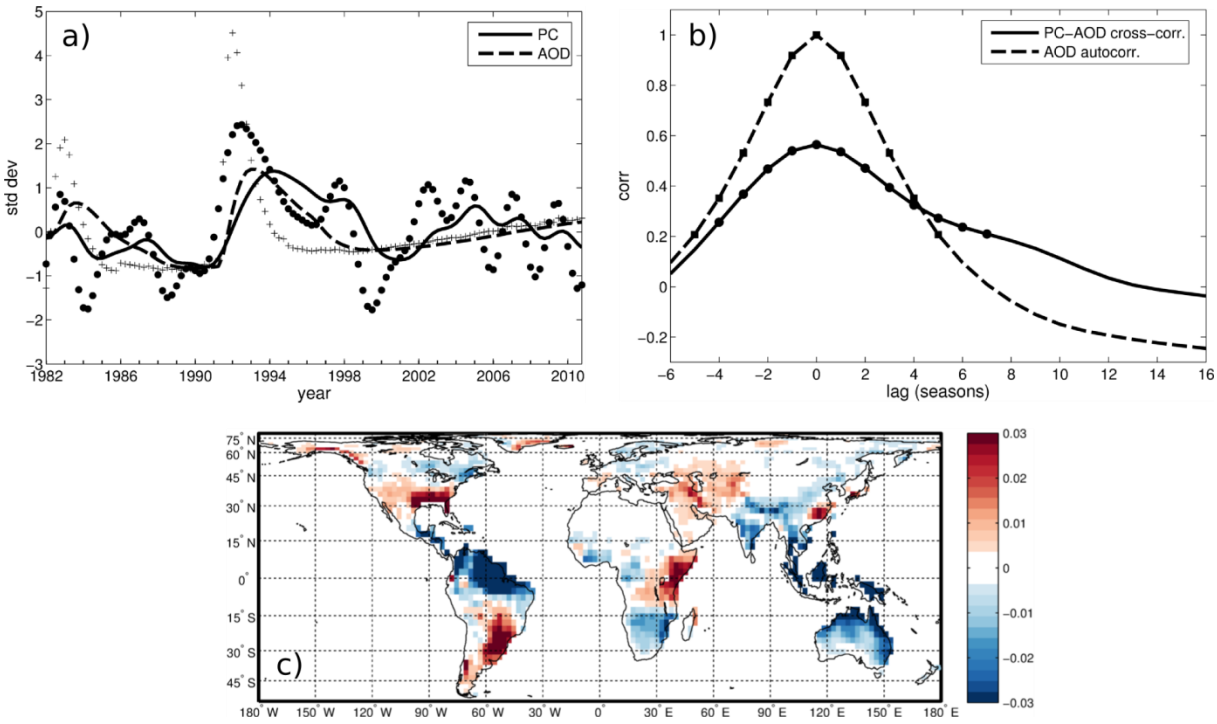

Figure 3. (a) First normalized PC of the PRE anomalies forced by the SM (full line and filled circles), after cutoff low-pass filtering at 2 year-1 frequency. Dashed line (and cross marks) stands for the normalized stratospheric Aerosol Optical Depth (AOD). Lines stand for 5-years exponential moving average while marks represent each single season. (b) Lagged correlations between AOD and PC1 of the forced PRE. The dashed curve is the autocorrelation function of the AOD. Marks indicate significance at the 5% level. (c) First EOF of the forced PRE. Arbitrary units.

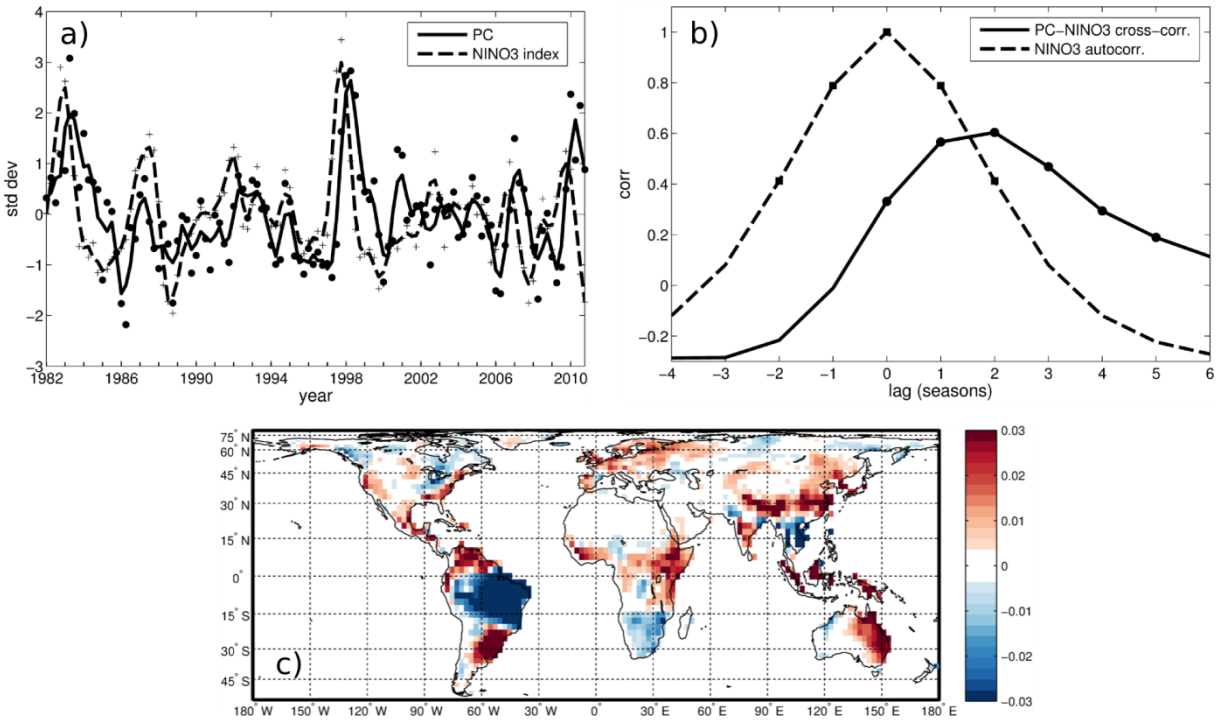

Figure 4. (a) Second normalized PC of the PRE anomalies forced by the SM (full line and filled circles). Dashed line (and cross marks) stands for the normalized NINO3 index. Lines stand for 3-seasons running means while marks represent each single season. (b) Lagged correlations between NINO3 index and PC1 of forced PRE. The dashed curve is the autocorrelation function of the NINO3 index. Marks indicate significance at the 5% level. (c) Second EOF of the forced PRE. Arbitrary units.

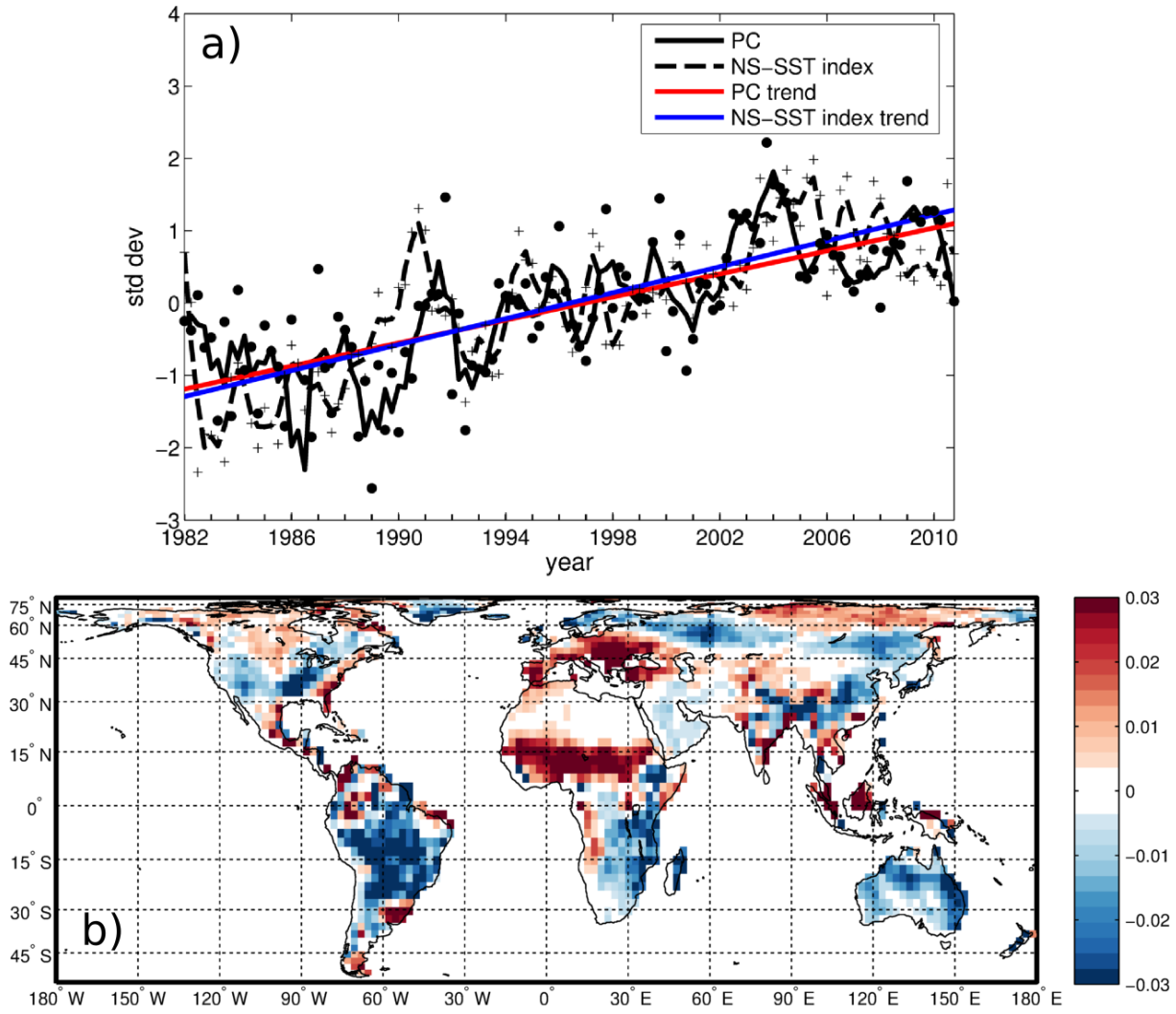

Figure 5. (a) Third normalized PC of the PRE anomalies forced by the SM (full line and filled circles). Dashed line (and cross marks) stands for the normalized NS-SST index. Lines stand for 3-seasons running means while marks represent each single season. Coloured lines represent the trends (red for the PC, blue for the NS-SST index). (b) Third EOF of the forced PRE . Arbitrary units.

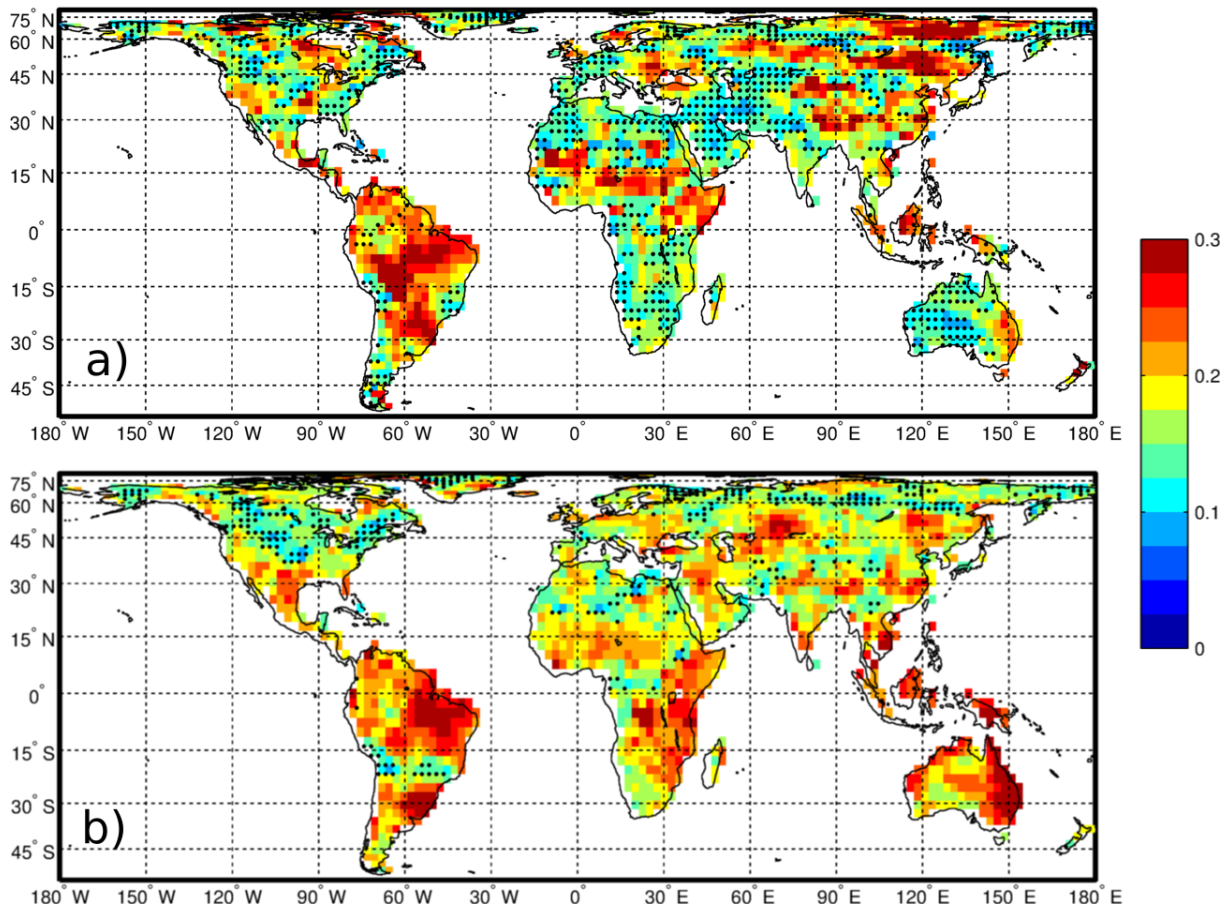

Figure 6. Ratio of the forced variance to the total variance. (a) The fraction of PRE variance forced by the SM which is also forced by the ET. (b) The fraction of PRE variance forced by the SM which is also forced by the LAI. Dots are placed over areas where variance ratio values did not pass a significance test at the 1% level.

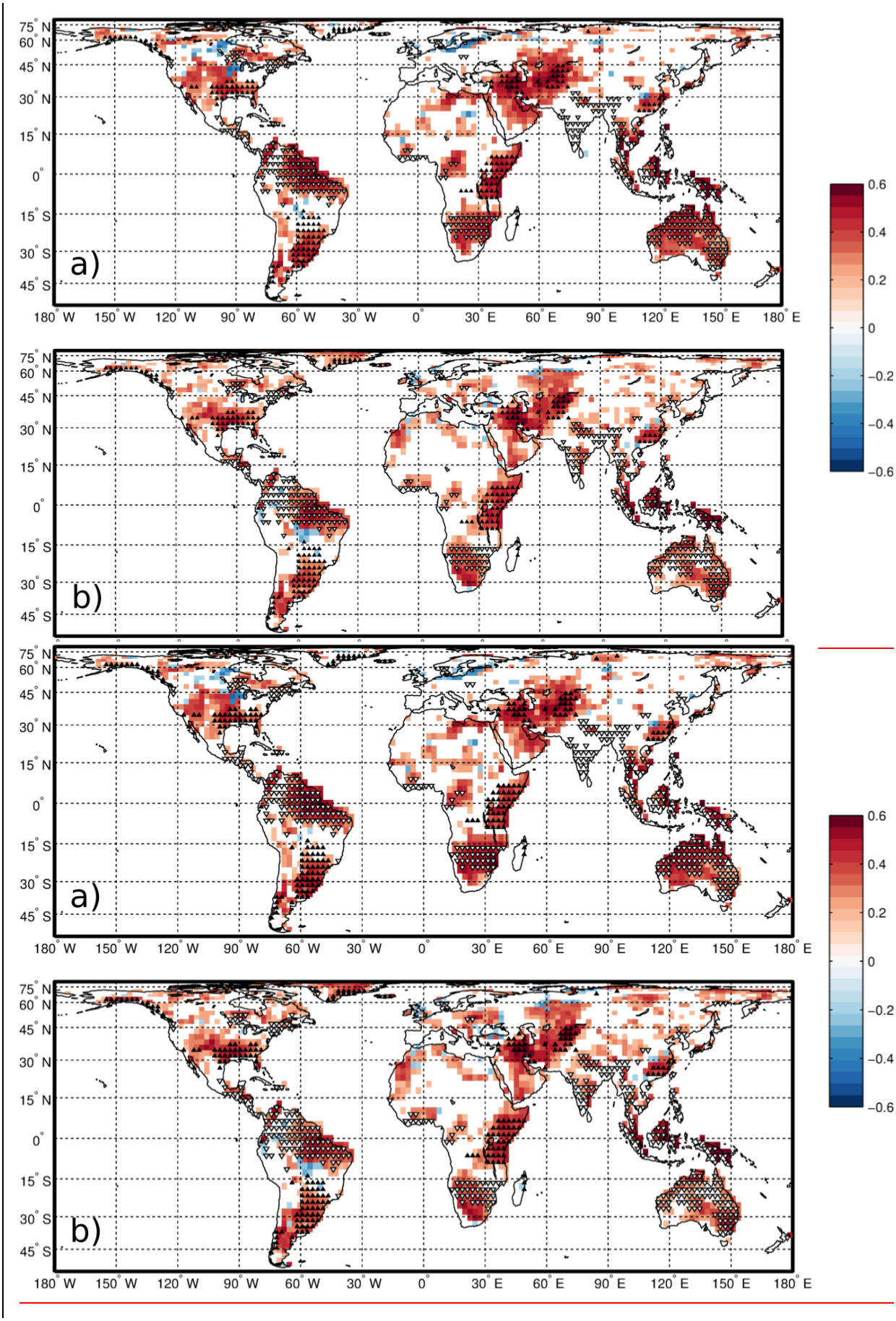
a)
b)
a)
b)
75° N
60° N
45° N
30° N
15° N
0°
15° S
30° S
45° S
180° W
150° W
120° W
90° W
60° W
30° W
0°
30° E
60° E
90° E
120° E
150° E
180° E
0.6
0.4
0.2
0
−0.2
−0.4
−0.6

1

2

Figure 7. Point-by-point correlation of the first mode of variability of PRE forced by SM with (a) the total fields of PRE forced by ET and (b) the PRE forced by LAI. Data have been filtered using a cutoff low-pass filter at 1 year frequency. Only areas where correlations passed a significance test at the 5% level are shown. Black upward (white downward) triangles denote areas with positive >0.01 (negative <-0.01) values of the first EOF of the PRE anomalies forced by the SM (Fig. 3c).

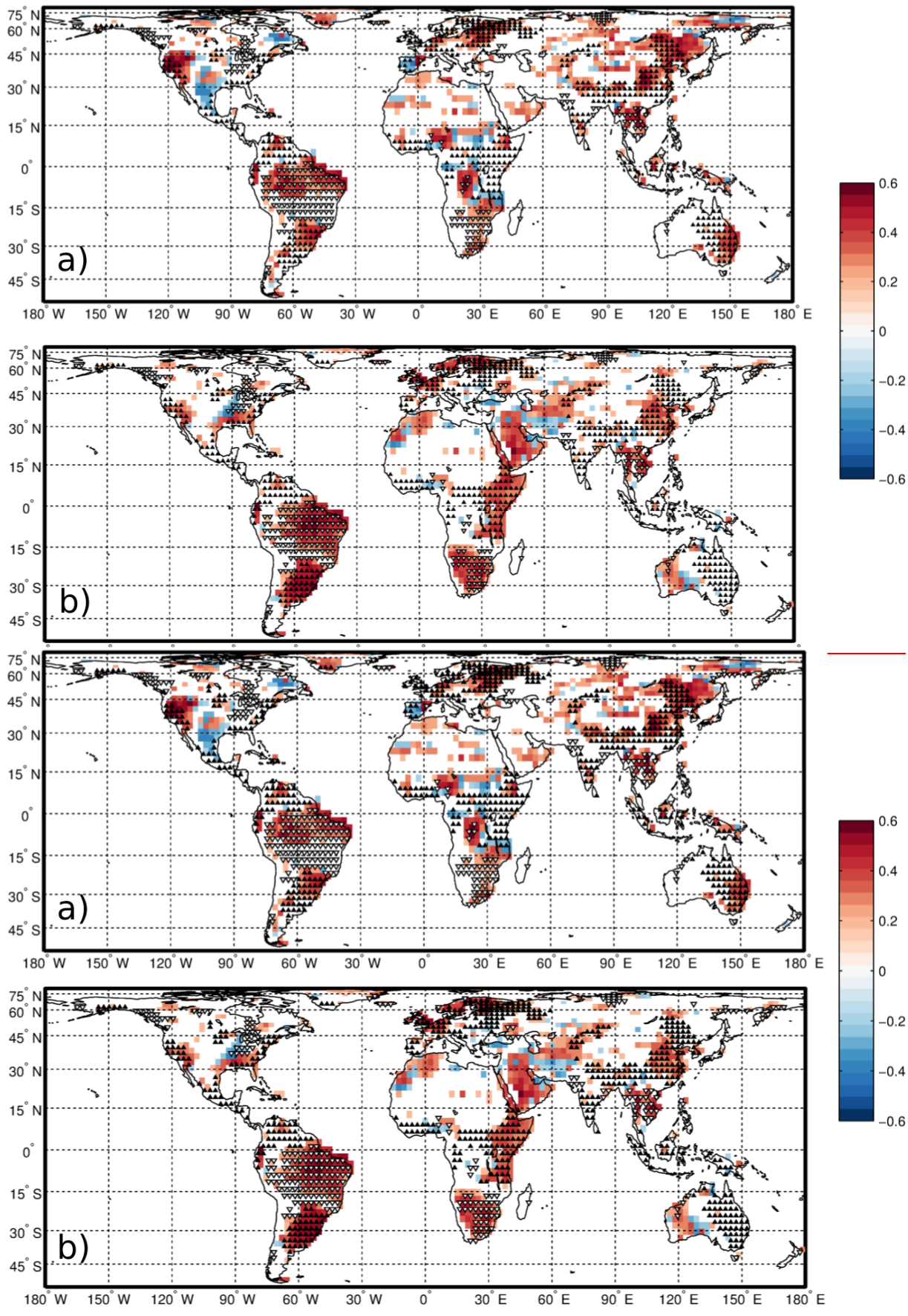
a)
b)
a)
b)
75° N
60° N
45° N
30° N
15° N
0°
15° S
30° S
45° S
180° W
150° W
120° W
90° W
60° W
30° W
0°
30° E
60° E
90° E
120° E
150° E
180° E
0.6
0.4
0.2
0
−0.2
−0.4
−0.6

Figure 8. Point-by-point correlation of the second mode of variability of PRE forced by SM with (a) the total fields of PRE forced by ET and (b) the PRE forced by LAI. Data have been filtered using a cutoff low-pass filter at 1 year frequency. Only areas where correlations passed a significance test at the 5% level are shown. Black upward (white downward) triangles denote areas with positive >0.01 (negative <-0.01) values of the second EOF of the PRE anomalies forced by the SM (Fig. 4c).

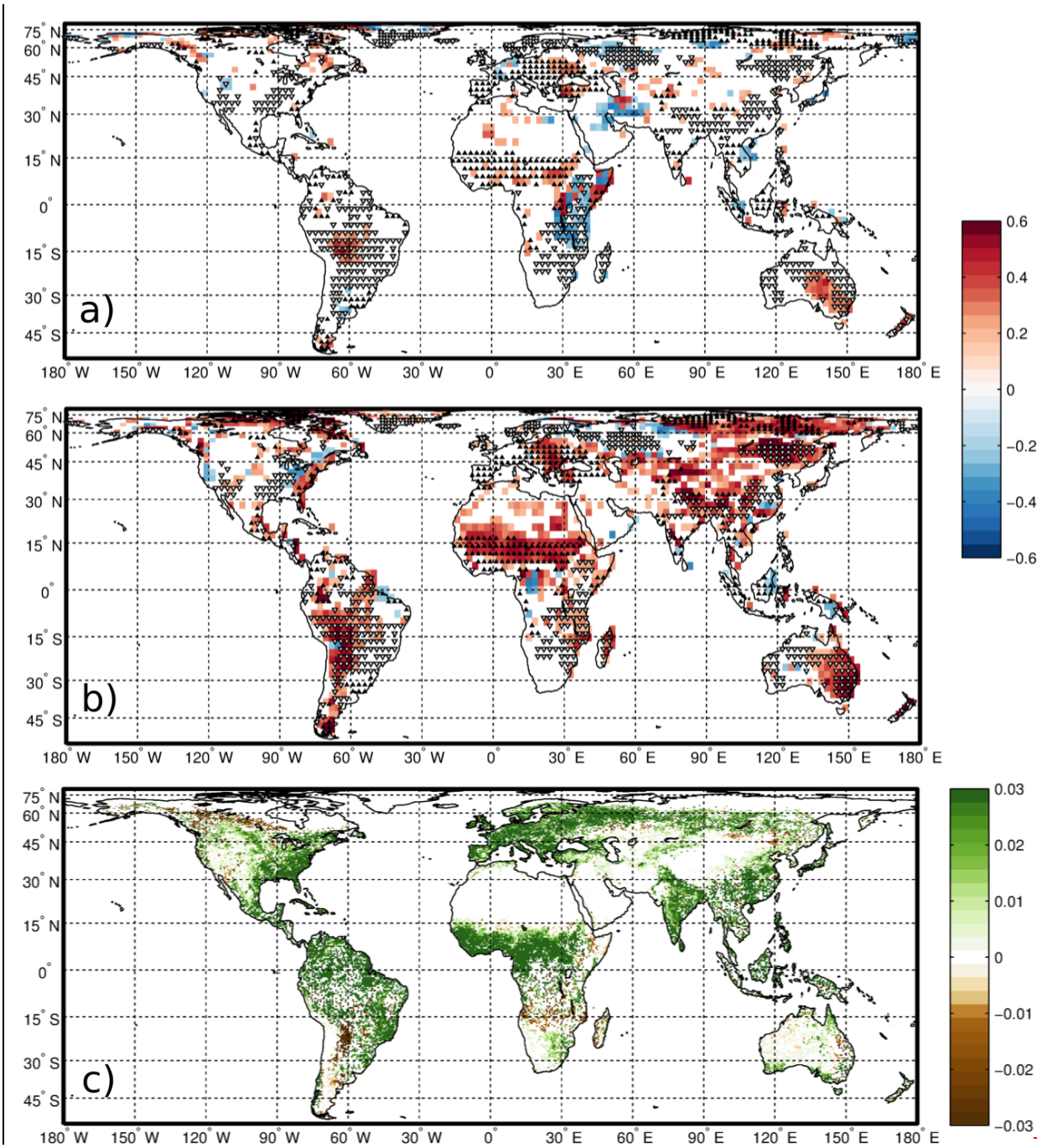
a)
b)
c)
75° N
60° N
45° N
30° N
15° N
0°
15° S
30° S
45° S
180° W
150° W
120° W
90° W
60° W
30° W
0°
30° E
60° E
90° E
120° E
150° E
180° E
0.6
0.4
0.2
0
−0.2
−0.4
−0.6
0.03
0.02
0.01
0
−0.01
−0.02
−0.03

1

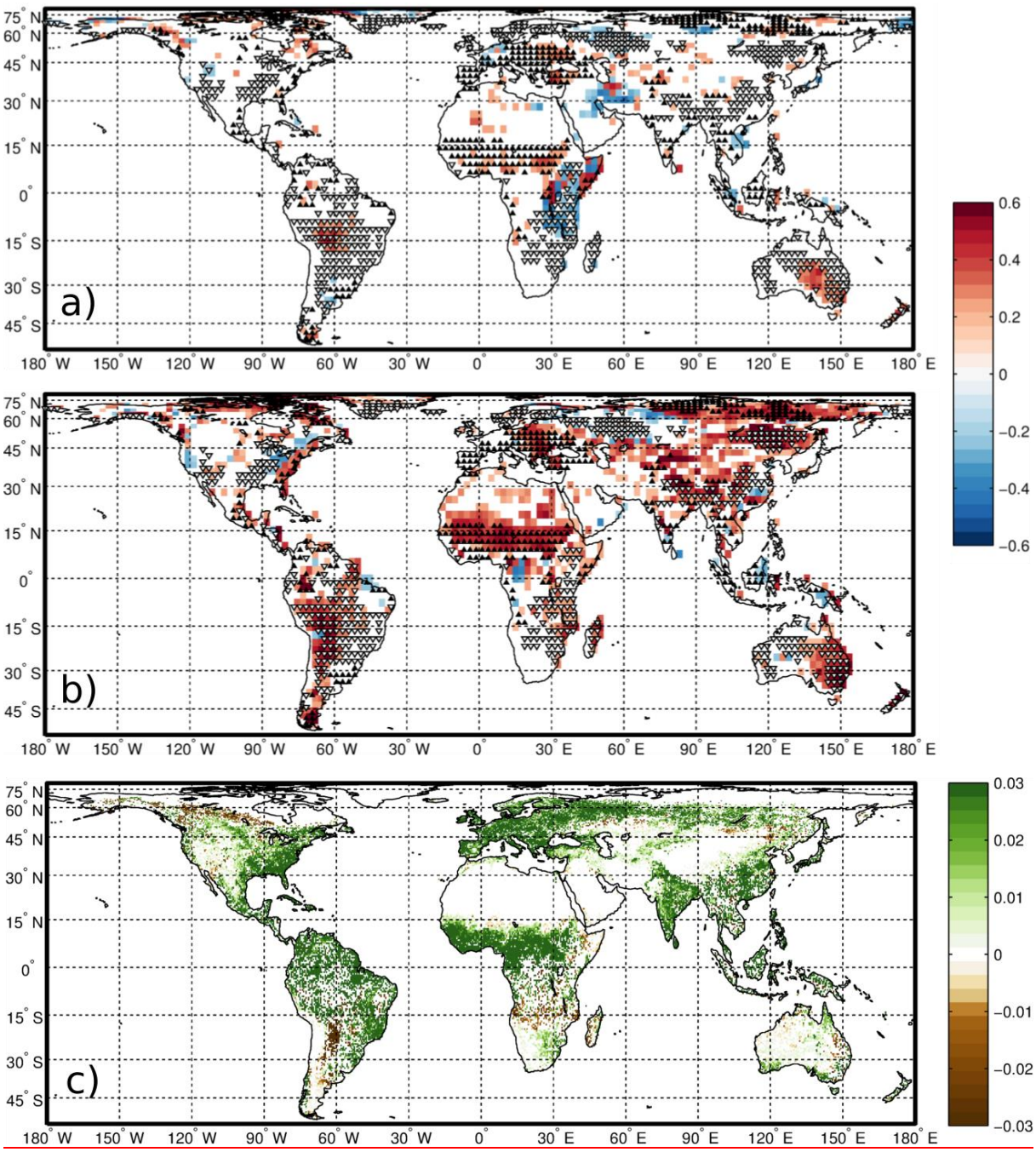

Figure 9. Point-by-point correlation of the third mode of variability of PRE forced by SM on the total field of (a) PRE forced by ET and (b) PRE forced by LAI. (c) Magnitude of the LAI change over 1982-2010, quantified using a linear model under the assumption of monotonic change. Data have been filtered using a cutoff low-pass filter at 1 year-1 frequency. Only areas where correlations (panels a-b) and trend (panel c) passed a significance test at the 5% level are shown. Black upward (white downward) triangles denote areas with positive >0.01 (negative <-0.01) values of the third EOF of the PRE anomalies forced by the SM (Fig. 5b).